

NATIONAL RESEARCH COUNCIL OF CANADA

**CIRCULATION AND DISTORTION OF LIQUID DROPS
FALLING THROUGH A VISCOUS MEDIUM**

REPORT NO. MT-22

BY

P. SAVIC

DIVISION OF MECHANICAL ENGINEERING

OTTAWA

31 JULY 1953

**THIS REPORT MAY NOT BE PUBLISHED IN WHOLE OR
IN PART WITHOUT THE WRITTEN CONSENT OF
THE NATIONAL RESEARCH COUNCIL**

UB/TIB Hannover 89

117 600 92X



NATIONAL RESEARCH LABORATORIES

Ottawa, Canada

REPORT

Division of Mechanical Engineering

Gas Dynamics Section

Pages - Preface - 6
Text - 35
App. - 7
Figures - 14

Report: MT-22
Date: 31 July 1953
Lab. Order: 6118A
File: M2-17-13.L-2

For: Internal

Subject: CIRCULATION AND DISTORTION OF LIQUID DROPS
FALLING THROUGH A VISCOUS MEDIUM

Submitted by: D.C. MacPhail
Section Head *DCM*

Author: P. Savic *P.S.*

Approved by: J.H. Parkin
Director *JHP*

SUMMARY

Existing theories of circulation in drops moving through a viscous medium are examined and found to be at variance with observation on water drops moving in castor oil. It is concluded that the suppression of circulation in small drops is due to a surface active layer, the extent of which is governed by the balance between interfacial tension and the integral of viscous surface shear. The streamline picture and the relation between size of surface layer and drag are found to be in good agreement with experiments, but the critical drop radius for transition from non-circulating to circulating condition is found to be somewhat lower than predicted.

The shape of a distorted drop suspended in a gas stream is calculated and found to be in general qualitative agreement with experiments in a vertical wind tunnel. The difference in wind velocity for breakup between a steady and

a suddenly applied gas stream, at least for very small drops, is ascribed to a higher rate of distortion under purely potential motion assumed to exist during a sudden blast. This assumption is shown to agree well with published experimental evidence.

In the appendix the development from rest of circulation in a drop is calculated for two conditions, viz., when the internal viscosity is high and when it is low compared with the viscosity of the surrounding fluid. It is shown that the time required to attain full circulation in the first case is over four times that in the second case. A numerical example of a kerosine spray in a combustion chamber shows that circulation may be a factor liable to affect the assessment of ignition delay times.

TABLE OF CONTENTS

| | <u>Page</u> |
|--|-------------|
| SUMMARY | (i) |
| LIST OF SYMBOLS | (v) |
| 1.0 INTRODUCTION | 1 |
| 2.0 CIRCULATION UNDER SURFACE TRACTION | 2 |
| 3.0 EXPERIMENTAL PROCEDURE | 6 |
| 4.0 CIRCULATION UNDER A STAGNANT MONOLAYER | 8 |
| 5.0 THE NATURE OF THE SURFACE LAYER | 24 |
| 6.0 DISTORTION OF A DROP IN A GAS STREAM | 26 |
| 7.0 CONCLUSIONS | 32 |
| 8.0 REFERENCES | 33 |

APPENDIX A: Development of Circulation from Rest by
Viscous Shear in the Vicinity of a Drop.

List of Illustrations

| | <u>Figure</u> |
|--|---------------|
| Water Drop in Castor Oil: | |
| Diameter 1.77 cm. | 1 |
| Diameter 1.21 cm. | 2 |
| Diameter 0.97 cm. | 3 |
| Diameter 0.74 cm. | 4 |
| Spherical Co-ordinates of Drop | 5 |
| Dependence of Total Drag on Central Angle of Stagnant Cap | 6 |
| Comparison of Actual and Theoretical Streamlines | 7 |

LIST OF ILLUSTRATIONS (Cont'd)

| | <u>Figure</u> |
|--|---------------|
| Surface Forces on Distorted Drop | 8 |
| Instability of Surface Layer Around Rear Stagnation Point | 9 |
| Hadamard's Constant vs. Non-dimensional Radius - Comparison Between Theory and Experiment | 10 |
| Distortion of Drop in a Gas Stream for Three Weber Numbers | 11 |
| Distorted Drop Suspended in Vertical Wind Tunnel | 12 |
| Dependence of Breakup Velocity Ratio on Droplet Radius | 13 |
| Growth of Strength of Circulation from Rest with Non-dimensional Time | 14 |

LIST OF SYMBOLS

| | |
|--------------------------|---|
| A | Radius of undistorted drop |
| a_n, A_n b_n, B_n | Constants of series expansions |
| c_n | Coefficients of Fourier expansion |
| C_n | Gegenbauer Polynomial of order n |
| D_r | Normal pressure drag |
| D_θ | Shear drag |
| D_n E_n F_n | Constant of series expansion |
| F_1, F_2 | Surface forces |
| g | Gravity acceleration |
| G_n H_n | Constants of series expansion |
| h | Exp. (Euler's constant) = 1.782.... |
| i | Imaginary unit |
| J | Sum of principal curvatures of surface |
| $J_0(t)$ | Bessel function of first kind of order zero |
| $K =$ | $-P_s/2N$ also Hadamard's constant |
| $L =$ | $-5\eta U/4AN$ |
| M_{mn} | Constants |
| m n | Integers |
| $N =$ | $3\eta U/2A$ |

LIST OF SYMBOLS (Cont'd)

| | |
|----------------------|---|
| p_{rr} | Normal stress |
| $p_{r\theta}$ | Shear stress |
| $P_n(y)$ | Legendre Polynomial |
| P_s | Static pressure difference on either side of surface |
| $q =$ | r/A |
| $Q_n(y)$ | Legendre function of second kind of order n |
| r | Radius vector, radial coordinate |
| s | Constant |
| t | Time |
| $u =$ | $-\gamma/2NA$ |
| U | Stream velocity at infinity |
| v_r | Radial velocity component |
| v_θ | Circumferential velocity component |
| W | Weber number $= \frac{1}{2}\rho_1 U^2 A / \gamma$ |
| $x_n =$ | $H_n A^{-n+1} U^{-1}$ or solutions of transcendental equation |
| $y =$ | $\cos\theta$ |
| α_1, α_2 | Areas on surface of drop |
| γ | Surface tension |
| γ' | Surface compression due to viscous traction |
| η | Viscosity |
| θ | Polar angle |
| ν | Kinematic viscosity |
| ρ | Density |
| ψ | Stream function |

CIRCULATION AND DISTORTION OF LIQUID DROPS FALLING THROUGH A VISCOUS MEDIUM

1.0 INTRODUCTION

1.1 This investigation was undertaken with a view to clearing up certain points in the theory of the motion of liquid drops through an atmosphere. In this respect two features of the problem were studied in detail, viz., circulation and distortion, the investigation being a preliminary to future research on heat transfer between atmosphere and drop and the impingement of drops on solid surfaces.

1.2 Circulation of the liquid in a drop has lately been recognized as being possibly an important factor influencing the heat transfer to the drop and its consequent evaporation or burning (in drops of liquid fuel), in that it promotes mixing of the liquid and hence accelerates the transmission of heat into the interior of the drop, while at the same time the moving surface of the circulating drop tends to decrease the thickness of the aerodynamic and thermal boundary layers. Kroning and Brink (Ref. 1) have demonstrated the effect on matter transfer to a circulating drop of the mixing inside the drop alone on the assumption that no boundary layer is formed. They showed that the time required to raise the concentration of the drop to about $2/3$ of the concentration of the surrounding fluid requires only about 40 percent of the time it takes pure diffusion to achieve this action. No estimation of the effect of the reduced boundary layer on the matter transfer time appears to have been made so far and may form the subject of a future study, but it is likely to increase the effect of circulation by another factor of possibly comparable order of magnitude. It will be realized that the effect of circulation on certain

practical phenomena such as ignition delay in combustion chambers or rate of evaporation of cooling sprays is likely to be important, and the conditions under which circulation is promoted or inhibited should therefore be ascertained. Here the situation is far from clear, as no satisfactory explanation seems to be in existence as to why small droplets should behave like solid spheres, i.e., should resist the surface traction of the surrounding medium while larger ones should circulate freely, thus reducing the drag by an appreciable amount. To shed light on this phenomenon, streamline photographs were taken of drops in the transition region from the "solid" to the "liquid" regime, and a theory was developed to account for this transition.

1.3 A theory of the distortion of a drop moving through a gas was developed to follow up the work of G.I. Taylor (Ref. 2), Lane, Prewett and Edwards (Ref. 3), and Golitzine (Ref. 4), and an attempt was made to account for the "bursting bag" mode of breakup of the drop. As a sequel to this theory, it was shown that the difference in critical velocity for breakup between a steady and a suddenly applied gas stream could be accounted for by reference to the gradual development of the boundary layer when the flow of gas is started from rest.

1.4 Finally, by way of Appendix A, it will be shown that a simple expression may be obtained for time taken by a drop to develop circulation after entering a viscous atmosphere. This part is included here as a further item which may conceivably influence ignition delay in such cases where circulation is physically possible.

2.0 CIRCULATION UNDER SURFACE TRACTION

2.1 A solution for the circulation in a liquid sphere moving in "creeping" motion through another fluid has been

obtained by Hadamard (Ref. 5) and Rybczinsky (Ref. 6). "Creeping" motion in this sense means low Reynolds number (about 0-1) flow whereby inertia forces are neglected relative to viscous stresses. This solution relates the circulatory motion of the fluid within the drop to the drag. The theory can therefore easily be checked by speed of descent measurements under gravity. Experimental results were at first disappointing as it was found that the drag for small droplets lay much closer to that given by Stokes for a rigid sphere than to the Rybczinsky-Hadamard solution. Arnold (Ref. 7) and others found that for large drops the drag approached the value of the Hadamard-Rybczynski theory, but in some cases never reached it. This may be partly due to the fact that in such cases distortion sets in before circulation is fully established or that the Reynolds number increases beyond the point below which the theory still applies. There seems, however, no obvious reason why circulation should cease below a certain radius of drop. Boussinesq (Ref. 8), realizing that surface tension and viscosity alone could not inhibit circulation, found it necessary to resort to introducing the concept of surface viscosity in order to account for the transition. Although no values of surface viscosity have yet been obtained by direct measurement, the attempt may be made to fit the observed rate-of-descent-drop radius curve by assuming suitable values for the surface viscosity. This, however, proves to be difficult, at least over part of the range. Bond (Ref. 9) and Bond and Newton (Ref. 10) have shown that for small drop radii the rate of descent of a drop is very close to the value given by Stokes' law for rigid spheres. With increasing radius the rate of descent at first remains in accordance with Stokes' formula until a certain critical radius is reached when the rate of descent changes comparatively rapidly and reaches Hadamard's value while the drop radius changes by only about 40 percent. This

is at variance with Boussinesq's theory which states that the transition from Stokes' to Hadamard's value is gradual. If the drag is given by:

$$D = 6\pi\eta_1 AUK \quad (1)$$

where A is the drop radius, η_1 is the viscosity of the fluid medium, and U the velocity of the drop relative to the medium, Hadamard's theory shows that K is given by:

$$K = \frac{2\eta_1 + 3\eta_2}{3\eta_1 + 3\eta_2} \quad (2)$$

where η_2 is the viscosity of the drop. Experimental results indicate that K is a function of A, varying from unity for small drops to the value in (2) for large ones. Weyssenhoff (Ref. 11) showed that Bond and Newton's curves of A versus K cannot be made to coincide with Boussinesq's as Bond and Newton demonstrated that K is almost constant for small values of A, while K in Boussinesq's theory increases monotonically with A.

2.2 The most important result of Bond and Newton's work is the fact that dynamic similarity seems to hold with the non-dimensional number

$$B = \frac{|\rho_1 - \rho_2| g A^2}{\gamma} \quad (3)$$

as the only significant parameter. Here ρ_1 is the density outside and ρ_2 inside the drop, g the gravitational acceleration and γ the surface tension. This result seems to indicate that either surface viscosity, if it exists, has no influence in promoting or inhibiting circulation, or that a separate (presumably molecular) relationship exists between surface viscosity and surface tension. Subsequent authors have tended to ignore the latter possibility and have assumed that surface tension alone was sufficient to account for the phenomenon. Garner (Ref. 12) leaves the question open but

relies on the significance of the Bond number (3) in describing the phenomenon. Hughes and Gilliland (Ref. 13) take up Bond and Newton's suggestion that, with high values of surface tension, circulation is prevented by the fact that in the front stagnation point of the drop the energy of the motion is partly expended in creating a new surface. They point out that, although an equal amount of surface is destroyed near the rear stagnation point, transmission of the energy from the rear to the front of the drop can only be truly loss free if the liquid were inviscid. Viscosity thus increases the energy loss manifesting itself in an increase in drag. They point out, however, that even when the drop radius is very small, circulation cannot be completely inhibited, since viscosity is a "linear" force. Hence, again it is difficult to see why the transition from Stokes' to Hadamard's regime should be as sudden as Bond and Newton found it to be.

2.3 It is clear, therefore, that unless the motion in the transition region were studied in greater detail, not many conclusions can be drawn from the available experimental evidence. It was not until recently that the motion inside the drop began to be studied. Garner obtained photographs of circulating drops but the order of magnitude within which he worked was one wherein the drops were considerably distorted and his results are therefore not suitable for comparison with theory. Spells (Ref. 14) recently obtained very clear photographs of the streamlines inside drops moving through another liquid making use of the schlieren pattern produced by imperfectly mixed water-glycerine mixtures, a method first used by Hagerty (Ref. 15). No worker in this field, however, seems to have obtained streamline visualizations within the transition region, and it was therefore decided to carry out experiments with a view to determining the exact mode of flow inhibition within the drop.

3.0 EXPERIMENTAL PROCEDURE

3.1 To visualize the streamlines in a drop, the method of light reflection from suspended particles was resorted to. Because of the large, very nearly spherical drops available by Bond and Newton's choice of water drops in castor oil, this combination was used, the flow inside the drop being made visible by suspended aluminium particles. Because of their tendency to float on the surface, it was difficult to suspend the particles directly, and it was found necessary first to make up a solution of polyvinyl alcohol in water into which the particles were mixed in considerable concentration while the solution was heated to boiling point and shaken. This concentrated suspension was then suitably diluted with distilled water. The small proportion of polyvinyl alcohol (less than 0.1 percent) being non-surface active should not have modified the properties of the pure water to any measurable extent.

The water drops were released from a glass drop tube whose end extended just under the surface of the castor oil. The actual drop tank was a square box with two brass plate sides and bottom and two opposite sides of 1/4-in. plate glass, the size being 8 by 8-1/2 by 18 in. One of the brass sides had a 1/4-in. broad slot milled down the centre with a plate glass strip sealed over it. A beam of light about 4 in. wide and 1/16 in. broad was thrown through this narrow window into the tank from a 500-watt spot light in such a way as to illuminate a section of 1/16-in. width through the centre of the drop. The light reflected from the suspended aluminium particles made visible the flow in the central section of the drop; and, by photographing through one of the plate glass sides in a direction at right angles to the beam of light, choosing a suitable exposure, the streamlines were made visible as short bright tracks against a dark background. For a detailed comparison with theory,

however, it was necessary to record the streamlines as seen by an observer travelling with the drop. To achieve this, the camera was mounted on the end of the piston rod of a hydraulic jack from which oil was forced through a fine control valve under a piston load of about 40 lb. This assured a smooth and easily regulated descent of the camera. A sighting telescope mounted on the camera was focused on the edge of the drop. It required very little practice in operating the oil valve to insure that the camera and water drop descended at the same rate. During the passage of the drop through the narrow beam of light the camera shutter was opened for a known time and the plate exposed. In this way, Figures 1 to 4 were obtained.

3.2 For large drop radii the stream line picture was found to be very nearly identical with Hadamard's solution for which also the drag was in good agreement. With drops of smaller diameter, the vortex ring appeared to be further forward in the drop and the whole picture ceased to be symmetrical about the horizontal equator. This might be expected to occur if the motion entered into the Oseen regime, but this would only happen if the drop radius increased. A further observation showed that a stagnant cap appeared to develop in the upper region of the drop with a fairly well defined edge at which the circumferential streaming motion came to an abrupt stop. With still smaller drops, this cap was larger; and, for the smallest drops, it enveloped the whole drop. When this occurred, the motion had reached the stage of the Stokes' law regime, and the internal circulation had altogether ceased.

3.3 This sequence of events will be seen to be at variance with Boussinesq's "surface viscosity" hypothesis, as in this case the motion cannot become asymmetrical. It is also incompatible with Hughes and Gilliland's interpretation of the interaction of viscosity and surface tension. For,

if the circulatory motion is inhibited by the energy expended in creating new surface, it is difficult to see why the motion should first stop near the rear stagnation point where energy is being generated by the disappearance of surface. At any rate it is inconceivable why surface energy should be exchanged at all since no net change of surface takes place anywhere but only an exchange of particles constituting the surface. As surface tension or surface energy has nothing to do with the identity of otherwise undifferentiated molecules, energy exchanges cannot be invoked to explain the observable facts.

3.4 Since none of the existing theories appeared to fit the observations, it was decided to develop a new theory which will be discussed in the following:

4.0 CIRCULATION UNDER A STAGNANT MONOLAYER

Briefly, the proposed theory may be outlined as follows:

4.1 A relatively incompressible surface layer is formed, which over a portion of the surface inhibits transmission of the viscous surface traction from the external medium into the liquid of the drop. Whether this layer is made up of molecules of surface active impurities or of oriented molecules of the bulk fluid is immaterial at the moment and will be discussed below. To the normal interfacial tension in this layer must be added the integrated effect of the surface tractions due to the outside fluid, but with opposite sign. The total tension in this layer is therefore a minimum at the rear stagnation point where at the same time the viscous outward suction is a maximum. The drop will therefore distort in the manner of the familiar "drop" shape observable in the initial stages of the motion. As the speed of the drop increases and with it the viscous suction, the surface layer becomes unstable and folds up at the rear stagnation point, its constituent particles being rapidly sucked away

into the surrounding fluid. This trailing filament has been observed by Arnold (Ref. 7) who also states that in some cases the liquid in the filament breaks up into smaller droplets. Thus the extent of the original surface layer is quickly reduced and if it cannot be regenerated sufficiently rapidly it will reach a stable size at which the viscous suction is just below that required to cause instability. The motion will therefore become stationary with a stagnant cap determining the drag of the drop as a function of its radius.

4.2 One may attempt mathematical formulation of this state of affairs by calculating the stream function for a motion with mixed boundary conditions. While the radial velocity is everywhere zero on the surface of the drop (the frame of reference being at rest relative to the drop), the circumferential velocity is only zero over the extent of the stagnant cap, being finite outside it. Owing to the small magnitude of the viscosity of the drop relative to the surrounding medium (in the case of water in castor oil the ratio at room temperature is about 1:1000), the surface traction over the surface not covered by the cap may be assumed zero while on the cap it remains finite. The solution of this boundary value problem will be attempted in the following section:

4.3 In "creeping motion" where inertia forces can be neglected, Stokes' stream function ψ is a solution of the equation:

$$\left[\frac{\partial^2}{\partial r^2} + \frac{1-t^2}{r^2} \frac{\partial^2}{\partial t^2} \right]^2 \psi = 0 \quad (4)$$

where $t = \cos\theta$. The boundary conditions are:

- (a) $v_r = 0$ for $r = A$ and all values of θ
- (b) $v_\theta = 0$ for $\theta_0 < \theta < \pi$ or $-1 < t < t_0$
- (c) $p_{r\theta} = \eta \left(\frac{\partial v_\theta}{\partial r} - \frac{v_\theta}{r} \right) = 0$ for $0 < \theta < \theta_0$ or $t_0 < t < +1$

(5)

here $p_{r\theta}$ is the circumferential viscous shear or surface traction, v_θ the circumferential velocity and v_r the radial velocity (Fig. 5). This problem could be solved by means of the general spherical harmonic expansions described by Lamb (Ref. 16), but here a more direct approach will be adopted involving a different set of orthogonal functions known as Gegenbauer or ultraspherical polynomials (Ref. 17). In (4) put

$$\left[\frac{\partial^2}{\partial r^2} + \frac{1-t^2}{r^2} \frac{\partial^2}{\partial t^2} \right] \psi = y \quad \text{and} \quad \left[\frac{\partial^2}{\partial r^2} + \frac{1-t^2}{r^2} \frac{\partial^2}{\partial t^2} \right] y = 0$$

and assume the product form of the solution: $y = r^n Z(t)$. The function $Z(t)$ now satisfies the ordinary second order differential equation:

$$Z''(1-t^2) + Z n(n-1) = 0 \quad (6)$$

The solution of (6) is the Gegenbauer or ultraspherical polynomial $C_n^{-\frac{1}{2}}$ of order n (see, for example, Magnus and Oberhettinger, Ref. 7). The corresponding solution of the fourth order equation (4) is now:

$$\psi = \sum_{n=2}^{\infty} C_n^{-\frac{1}{2}} (A_n r^n + B_n r^{1-n} + C_n r^{n+2} + D_n r^{3-n}) \quad (7)$$

To get the correct stress condition, the solution pertaining to the outside fluid must be sought. The velocity components are given by:

$$v_\theta = \frac{1}{r \sin \theta} \frac{\partial \psi}{\partial r} \quad \text{and} \quad v_r = - \frac{1}{r^2 \sin \theta} \frac{\partial \psi}{\partial \theta} \quad (8)$$

Hence on the surface of the drop:

$$v_{\theta} = \sum_{n=2}^{\infty} \frac{C_n^{-\frac{1}{2}}}{\sin\theta} (E_n A^{n-2} + F_n A^{-n-1} + G_n A^n + H_n A^{1-n})$$

The constants in this expression are connected with those in (7) via the circumferential velocity (8). Hence for the solution outside the sphere: $E_n = G_n = 0$ except for $E_2 = 2U$ to satisfy conditions at infinity. Condition 5(a) is satisfied provided:

$$F_n = \frac{H_n (1 - n)}{(n - 3)} A^2$$

Thus it follows that:

$$v_{\theta} = \sum_{n=3}^{\infty} \frac{C_n^{-\frac{1}{2}}}{\sin\theta} H'_n \left[A^2 (1 - n) r^{-n-1} + (n - 3) r^{1-n} \right] + \left[2U + (UA^3 + H'_2 A^2) r^{-3} + H'_2 r^{-1} \right] \frac{C_2^{-\frac{1}{2}}}{\sin\theta} \quad (9)$$

where $H'_n = \frac{H_n}{n - 3}$.

4.4 In order to satisfy the remaining conditions 5(b) and 5(c) use has to be made of the orthogonality property of the Gegenbauer polynomials, viz.

$$\int_{-1}^{+1} \frac{C_m^{-\frac{1}{2}} \cdot C_n^{-\frac{1}{2}}}{1 - t^2} dt = \begin{cases} 0 & \text{for } m \neq n \\ \frac{1}{n(n-1)(n-\frac{1}{2})} & \text{for } m = n \end{cases}$$

Multiplying (9) by $C_m^{-1/2}$, dividing by $\sin\theta$ and integrating with respect to t from -1 to $+1$ and with the aid of the orthogonality property, one obtains:

$$\begin{aligned} \int_{-1}^{+1} \frac{v_\theta C_m^{-1/2}}{1-t^2} dt &= - \frac{2H'_n A^{1-m}}{m(m-1)(m-\frac{1}{2})} = \int_{t_0}^{+1} \frac{r \frac{\partial v_\theta}{\partial r} C_m^{-1/2}}{1-t^2} dt \\ &= 4 \sum_{n=3}^{\infty} (n-1) A^{1-n} H'_n \int_{t_0}^{+1} \frac{C_n^{-1/2} C_m^{-1/2}}{1-t^2} dt \\ &\quad - (3U + 4H'_2 A^{-1}) \int_{t_0}^{+1} \frac{C_2^{-1/2} C_m^{-1/2}}{1-t^2} dt \end{aligned} \quad (10)$$

This is a system of linear equations determining the coefficients H_n . To facilitate notation, put:

$$\int_{t_0}^{+1} \frac{C_n^{-1/2} C_m^{-1/2}}{1-t^2} dt = M_{mn}$$

and

$$H_n A^{-n+1} U^{-1} = x_n$$

The equation (10) can be written in the following manner:

$$\begin{aligned} x_2(-2/3-4M_{22})+8x_3M_{23}+12x_4M_{24}+16x_5M_{25}+20x_6M_{26}+24x_7M_{27}+\dots &= 3M_{22}+1 \\ -4x_2M_{32}+x_3(2/15+8M_{33})+12x_4M_{34}+16x_5M_{35}+20x_6M_{36}+24x_7M_{37}+\dots &= 3M_{32} \\ -4x_2M_{42}+8x_3M_{43}+x_4(1/21+12M_{44})+16x_5M_{45}+20x_6M_{46}+24x_7M_{47}+\dots &= 3M_{42} \\ -4x_2M_{52}+8x_3M_{53}+12x_4M_{54}+x_5(1/45+16M_{55})+20x_6M_{56}+24x_7M_{57}+\dots &= 3M_{52} \\ \dots\dots\dots &\dots\dots\dots \\ \dots\dots\dots &\dots\dots\dots (11) \end{aligned}$$

The labour in solving this numerical problem to a high degree of accuracy would be prohibitive, therefore only six terms were determined using six of the equations (11) to determine the unknown coefficients x_n of order 2 to 7. In finding the values of the integrals M_{mn} , it is useful to remember that the Gegenbauer polynomials are connected with the Legendre polynomials P_n by the relation:

$$C_n^{-\frac{1}{2}} = \frac{1}{2n-1} (P_{n-2} - P_n) \quad (12)$$

Equations (11) were solved for a number of cap angles θ_0 varying between 0 and 180 degrees corresponding to various conditions within the transition region.

4.5 Having found the coefficients x_n , the next step is to calculate the drag of the drop for various cap angles. The drag is the sum of two components, viz., the shear drag D_θ and the normal pressure drag D_r . The former is calculated from the tangential surface shear $p_{r\theta}$ given by:

$$p_{r\theta} = \eta \left(\frac{\partial v_\theta}{\partial r} - \frac{v_\theta}{r} \right)$$

integrated over the surface of the drop thus:

$$D_\theta = \int_0^\pi 2A^2 \pi \sin^2 \theta p_{r\theta} d\theta$$

With the aid of (12) and the fact that:

$$\int_0^\pi P_n \sin \theta d\theta = 0 \quad \text{except for } n = 0 \text{ when it is } = 2, \text{ the shear}$$

drag turns out to be:

$$D_\theta = -8A\eta U \pi (1 + x_2) \quad (13')$$

The normal pressure drag may be calculated from the formula:

$$D_r = - \int_0^\pi 2A^2 \pi \sin\theta \cos\theta p_{rr} d\theta$$

where p_{rr} is the normal viscous stress on the surface of the drop defined by:

$$p_{rr} = -p + 2\eta \frac{\partial v_r}{\partial r}$$

Here p is the mean pressure which may be obtained from the reduced Stokes'-Navier equation:

$$\text{grad } p = \eta \text{ div grad } \vec{v}$$

From this is obtained:

$$p_{rr} = \frac{\eta U}{A} \left[- (6 + 3x_2) P_1 + 6 \sum_{n=3}^{\infty} \frac{x_n P_{n-1}}{n} \right] \quad (14')$$

Hence D_r is found to be:

$$D_r = 4\pi\eta A (2 + x_2)$$

and together with (13') the total drag D is:

$$D = D_r + D_\theta = -4\pi\eta A x_2 \quad (15')$$

It will be seen that the drag depends only on the first coefficient x_2 of the expansion. This is convenient as this coefficient is likely to be the most accurate one as will be realized from the manner in which these coefficients were obtained. Figure 6 shows the dependence of x_2 and hence of the drag on the central angle θ_0 of the cap. To compare this

formula with experiment, the radii of the drops were measured as well as their rate of descent and the central angle of the cap was estimated from the photographs. The results of this comparison are compiled in Table I.

TABLE I

| Radius of Drop A (cm.) | $U_{\text{exp.}}$ cm./sec. | $U_{\text{cal.}}$ cm./sec. |
|---------------------------|-------------------------------|-------------------------------|
| 0.89 | 1.16 | 1.22 |
| 0.605 | 0.62 | 0.62 |
| 0.49 | 0.25 | 0.29 |
| 0.37 | 0.13 | 0.15 |

The drag was put equal to $\frac{4}{3} A^3 \pi (\rho_1 - \rho_2) g$. This gave an expression for the fall velocity $U_{\text{cal.}}$. Considering the difficulty in accurately measuring the cap angle and the fact that the drop radius enters the formula in the second power, the agreement is considered sufficiently good to show that no forces other than those assumed are involved in the phenomenon.

4.6 To find the stream function relevant to the internal flow ψ_1 the coefficients E_n and G_n must be found, in the expansion for v_θ , while all F_n and H_n are zero. At the boundary the expansion must be equal to (9). From this condition the values of E_n and G_n are found by equating terms of equal order n . Using the first of relations (8) the stream function is found to be:

$$\psi_1 = -UA^2 C_2^{-\frac{1}{2}} \left(\frac{3}{2} + x_2 \right) (R^2 - R^4) + UA^2 \sum_{n=3}^{\infty} C_n^{-\frac{1}{2}} x_n (q^n - q^{n+2}) \quad (13)$$

where $q = r/A$. A streamline plot has been obtained from this expression using equal increments of the non-dimensional stream

function ψ_1/UA^2 . The result is shown on Figure 7 on the right half while on the left half was plotted a reproduction of the streamlines from an actual photograph with similar central angle of cap (approx. 120°). The general agreement is reasonable considering that only six terms were taken in the expansion.

4.7 Next, the attempt will be made to calculate the falling speed in its relation to drop radius. This is the function plotted by Newton and Bond (Ref. 10) and presents the most straightforward indication of transition, and one that is most easily measured.

4.8 The forces acting on the cap and tending to fold it up at the rear stagnation point may be calculated on the assumption that in the stable position their intensity is just below the level necessary to fold up the surface layer at the rear stagnation point. Suppose the distorted droplet be given by the shape in Figure 8. Here $d\alpha_1$ and $d\alpha_2$ are two differential areas of the surface. It is assumed that the force dF_2 on $d\alpha_2$ is entirely due to the force dF_1 on $d\alpha_1$ transmitted along the surface. Then, at equilibrium, the principle of virtual displacements demands that:

$$dF_1 \cdot r_1 d\theta_1 = dF_2 \cdot r_2 d\theta_2$$

The two angular displacements $d\theta_1$ and $d\theta_2$ are connected by the condition that the two differential areas must be equal, i.e.

$$r_1^2 \sin\theta_1 \cdot d\theta_1 \cdot d\phi = r_2^2 \sin\theta_2 \cdot d\theta_2 \cdot d\phi$$

The force dF_1 is due to the surface traction $p_{r\theta}$,

$$dF_1 = p_{r\theta} r_1^2 \cdot \sin\theta_1 \cdot d\theta_1 \cdot d\phi$$

and hence the transmitted force dF_2 is given by:

$$dF_2 = r_2 \cdot \sin\theta_2 \cdot p_{r\theta} d\theta_1 \cdot d\phi$$

Thus the differential force per unit length $d\gamma'$ is:

$$d\gamma' = dF_2 / r_2 \sin\theta_2 d\phi = p_{r\theta} r_1 \cdot d\theta_1$$

If it is assumed that the surface layer below $d\alpha_1$ causes a surface compression while the area above it adds a term to the surface tension, the integrated effect of all surface tractions is:

$$\gamma' = \int_0^{\theta_1} p_{r\theta} \cdot r \cdot d\theta - \int_{\theta_1}^{\pi} p_{r\theta} r \cdot d\theta \quad (14)$$

This is the term which must at each point of the surface be subtracted from surface tension, when the distorted shape is being calculated. It follows from the definition of $p_{r\theta}$ that:

$$p_{r\theta} = \frac{\eta U}{A} \left[-6(1 + x_2) \frac{C_2^{-\frac{1}{2}}}{\sin\theta} + 2 \sum_{n=3}^{\infty} \frac{C_n^{-\frac{1}{2}}}{\sin\theta} x_n (2n - 1) \right] \quad (15)$$

4.9 To give an illustration of the stability calculations it will be assumed that initially the stagnant layer envelops the whole drop. In this case (15) reduces to:

$$p_{r\theta} = N \sin\theta \quad \text{where } N = \frac{3\eta U}{2A}$$

Moreover, the shape of the drop is supposed to be only slightly non-spherical, the distortion terms entering the calculations as first-order perturbations, i.e.,

$$r = A \left(1 + \sum_0^{\infty} a_n y^n \right) \quad \text{where } y = \cos\theta \quad (16)$$

The coefficients a_n are determined by pressure balance considerations on either side of the surface, as will be seen in the following, but in addition are restricted by the condition that the volume enclosed by the surface must remain constant whatever the distortion. Thus:

$$\text{Volume } V = \int_0^\pi \frac{2r^3\pi}{3} \sin\theta \cdot d\theta = - \frac{2A^3\pi}{3} \int_{+1}^{-1} \left(1 + 3 \sum_0^\infty a_n y^n \right) dy$$

Volume conservation requires:

$$\int_{+1}^{-1} \sum_0^\infty a_n y^n \cdot dy = 0 \quad (17)$$

Equation (14) can now be put in the form:

$$\gamma' = - \int_1^y NA \left(1 + \sum_0^\infty a_n y^n \right) dy + \int_y^{-1} NA \left(1 + \sum_0^\infty a_n y^n \right) dy \quad (18)$$

Since most of the distortion will be near the rear stagnation point, the net surface tension being a minimum there, attention will be confined to $y = -1 + \epsilon$ where ϵ is small. If it is assumed that the products $a_n \epsilon$ can be neglected, equation (18) can, with the aid of (17), be reduced to:

$$\gamma' = - 2yNA \quad (19)$$

The pressure discontinuity due to surface forces is therefore $J (\gamma + 2y \times NA)$, where J is the sum of principal curvatures. Taking only first order terms into account, this quantity can be expressed in term of (16) thus:

$$J = \frac{1}{A} \left(2 - \sum_0^\infty a_n (n-1) \left[ny^{n-2} - (n+2) y^n \right] \right) \quad (20)$$

The surface discontinuity is held in balance by the sum of static pressure difference P_s , viscous normal pressure p_{rr} , which from (14) is found to be $= \frac{5\eta Uy}{2A}$ and the gravity pressure $= (\rho_1 - \rho_2)g(r_0 + ry)$ where r_0 is obtained from (16) by putting $y = -1$. The assumption that both p_{rr} and $p_{r\theta}$ are not materially affected by distortion is probably not very accurate; but, in view of experimental evidence showing that distortion seems confined to higher order terms, it will be maintained. The pressure balance equation thus assumes the form:

$$J(\gamma + 2y \times NA) = P_s + (\rho_1 - \rho_2)g(r_0 + ry) + \frac{5\eta Uy}{2A} \quad (21)$$

4.10 One way of solving this equation would be to insert (16) and (20) into it and equate terms of equal order. It is easier, however, to expand the radius vector of the surface not, as in (16), as a power series of $\cos\theta$, but as a series of Legendre polynomials:

$$r = A \left[1 + \sum_{n=2}^{\infty} b_n P_n(y) \right] \quad (22)$$

In this form the volume conservation condition (17) is automatically satisfied. The sum of principal curvatures now assumes the form:

$$J = \frac{1}{A} \left[2 - \sum_{n=2}^{\infty} b_n P_n(y) (n+2)(n-1) \right] \quad (23)$$

Near the rear stagnation point the second term on the right side of (21) can be neglected, leaving:

$$2 - \sum_{n=2}^{\infty} b_n P_n(y) (n+2)(n-1) = \frac{K + Ly}{u - y} \quad (24)$$

where $K = -P_s/2N$, $L = -5\eta U/4AN$ and $u = -\gamma/2NA$.

To solve (24), the right side must be expanded in a series of Legendre polynomials. Multiplying (24) by P_m and integrating with respect to y between the limits -1 and $+1$, it will be seen that on the left side all terms vanish except for $m = n$ which term becomes $\frac{2b_n (n+2)(n-1)}{2n+1}$. Taking the first part of the right side, it will be seen that it transforms into the Neumann integral, viz:

$$K \int_{-1}^{+1} \frac{P_n(y)}{u-y} dy = 2K \cdot Q_n(u)$$

where $Q_n(u)$ is the Legendre function of the second kind of order n . The second term on the right of (24) can be dealt with by means of the recurrence relation for Legendre functions, viz:

$$yP_n = \frac{1}{2n+1} \left[(n+1) P_{n+1} + nP_{n-1} \right]$$

The resulting expression for the coefficients b_n is therefore:

$$b_n = - \frac{K (2n+1)}{(n+2)(n-1)} Q_n(u) - \frac{L}{(n+2)(n-1)} \times \left[(n+1) Q_{n+1}(u) + nQ_{n-1}(u) \right] \quad (25)$$

In accordance with usual practice, instability is defined as the condition under which one or more of the coefficients of the expansion becomes infinite or if all terms remain finite but the series itself starts to diverge. The former condition is attained when $u = 1$. To get a clearer picture of the nature of this instability, assume that u is only

slightly smaller than unity; in this case the dominant terms of Q_n are given by:

$$Q_n(u) \cong P_n(u) \cdot \tanh^{-1}u$$

It will be seen from (22) and (25) that even if $\lim (K+L) \tanh^{-1}u$ for $u \rightarrow 1$ remains finite, the series (22) will diverge logarithmically for $y = 1$. Thus, as expected, near the rear stagnation point the distortion will reach a maximum. For u very close to unity and on the assumption that both K and L are small, the series (22) may be summed approximately by replacing it by an integral. For large values of n , the coefficients (25) will assume the form:

$$b_n = -2 (K + L) \frac{P_n(u)}{n} \cdot \tanh^{-1}u \quad (26)$$

Now, from the addition theorem for Legendre polynomials it follows that:

$$P_n(u) P_n(y) = P_n(uy)$$

provided u and y are both very nearly unity. Thus, replacing the summation in (22) by an integral, the radius vector of the surface becomes:

$$r = A \left[1 - 2 (K + L) \cdot \tanh^{-1}u \int_1^\infty \frac{P_n(uy)}{n} dn \right] \quad (27)$$

This integral can be evaluated approximately by replacing P_n by its asymptotic value for large n , viz:

$$P_n(\cos\theta) \cong J_0(2n \sin\theta/2)$$

In evaluating this integral use may be made of the integral representation due to Lerch (see, for example, Magnus and Oberhettinger, "Special Functions of Mathematical Physics" chapt. III, para. 5).

$$\int_{2x}^{\infty} J_0(t) \frac{dt}{t} = \frac{-1}{4i\pi} \int_{-\frac{1}{2}-i\infty}^{-\frac{1}{2}+i\infty} \frac{\Gamma(-s) \cdot x^{2s}}{s\Gamma(s+1)} ds$$

where Γ = Euler's Gamma Function

J_0 = Bessel Function

Evaluating this integral by the method of residues, it will be seen that the integral of (27) for u very nearly = 1 is:

$$\int_1^{\infty} \frac{P_n(\cos\theta)}{n} dn \cong \log(h \sin\theta/2) + \sum_{k=1}^{\infty} \frac{(2 \sin\theta/2)^{2k}}{2^{k+1} \cdot k \cdot (k!)^2}$$

where $h = \exp. (\text{Euler's constant}) = 1.782\dots$. Near the stagnation point the second term on the right becomes small as the series converges very rapidly. Thus in this region (27) may be written as:

$$r = A \left[1 - 2 (K + L) \cdot \tanh^{-1} u \cdot \log (h \cdot \sin\theta/2) \right] \quad (28)$$

This equation shows that the influence of surface traction on the droplet will be a distortion in the shape of a thin filament of liquid being drawn from its rear stagnation region (Fig. 9). This filament can be observed in most liquid droplets moving through another liquid; in some cases, the filament breaks up into individual smaller droplets some distance away from the main drop.

slightly smaller than unity; in this case the dominant terms of Q_n are given by:

$$Q_n(u) \cong P_n(u) \cdot \tanh^{-1}u$$

It will be seen from (22) and (25) that even if $\lim (K+L) \tanh^{-1}u$ for $u \rightarrow 1$ remains finite, the series (22) will diverge logarithmically for $y = 1$. Thus, as expected, near the rear stagnation point the distortion will reach a maximum. For u very close to unity and on the assumption that both K and L are small, the series (22) may be summed approximately by replacing it by an integral. For large values of n , the coefficients (25) will assume the form:

$$b_n = -2 (K + L) \frac{P_n(u)}{n} \cdot \tanh^{-1}u \quad (26)$$

Now, from the addition theorem for Legendre polynomials it follows that:

$$P_n(u) P_n(y) = P_n(uy)$$

provided u and y are both very nearly unity. Thus, replacing the summation in (22) by an integral, the radius vector of the surface becomes:

$$r = A \left[1 - 2 (K + L) \cdot \tanh^{-1}u \int_1^\infty \frac{P_n(uy)}{n} dn \right] \quad (27)$$

This integral can be evaluated approximately by replacing P_n by its asymptotic value for large n , viz:

$$P_n(\cos\theta) \cong J_0(2n \sin\theta/2)$$

In evaluating this integral use may be made of the integral representation due to Lerch (see, for example, Magnus and Oberhettinger, "Special Functions of Mathematical Physics" chapt. III, para. 5).

$$\int_{2x}^{\infty} J_0(t) \frac{dt}{t} = \frac{-1}{4i\pi} \int_{-\frac{1}{2}-i\infty}^{-\frac{1}{2}+i\infty} \frac{\Gamma(-s) \cdot x^{2s}}{s\Gamma(s+1)} ds$$

where Γ = Euler's Gamma Function

J_0 = Bessel Function

Evaluating this integral by the method of residues, it will be seen that the integral of (27) for u very nearly = 1 is:

$$\int_1^{\infty} \frac{P_n(\cos\theta)}{n} dn \cong \log(h \sin\theta/2) + \sum_{k=1}^{\infty} \frac{(2 \sin\theta/2)^{2k}}{2^{k+1} \cdot k \cdot (k!)^2}$$

where $h = \exp.$ (Euler's constant) = 1.782.... Near the stagnation point the second term on the right becomes small as the series converges very rapidly. Thus in this region (27) may be written as:

$$r = A \left[1 - 2 (K + L) \cdot \tanh^{-1}u \cdot \log(h \cdot \sin\theta/2) \right] \quad (28)$$

This equation shows that the influence of surface traction on the droplet will be a distortion in the shape of a thin filament of liquid being drawn from its rear stagnation region (Fig. 9). This filament can be observed in most liquid droplets moving through another liquid; in some cases, the filament breaks up into individual smaller droplets some distance away from the main drop.

It may be concluded from the foregoing that the stagnant surface layer will become unstable as soon as the local integral of the surface tractions becomes equal to the interfacial tension between the two media. In general therefore:

$$\gamma' = \gamma \quad (29)$$

where γ' is given by (14). Thus at the rear stagnation point:

$$\gamma = A \int_0^{\pi} p_{r\theta} d\theta$$

Here r has been replaced by A , since the distortion is everywhere small except near the stagnation point. This expression may be calculated from (15), whereby the integration can be carried out by means of the relation:

$$\frac{C_n^{-\frac{1}{2}}(y)}{1 - y^2} = \frac{1}{n(n-1)} \frac{d}{dy} P_{n-1}(y)$$

Hence, (29) becomes explicitly:

$$\gamma = U\eta \left[-6(1 + x_2) + \sum_{n=4,6,8}^{\infty} \frac{4x_n(2n-1)}{n(n-1)} \right] \quad (30)$$

Suppose the drop is falling freely under the action of gravity and viscous drag, i.e.:

$$\frac{4}{3} \pi A^3 (\rho - \rho_1)g = 4\pi U A \eta x_2 \quad (31)$$

as the drag is given by (15'). Eliminating $U\eta$ between (30) and (31) the expression is obtained:

$$A^2 = 3\gamma x_2 / (\rho - \rho_1)g \left[-6(1 + x_2) + \sum_{n=4,6,8..}^{\infty} \frac{4x_n (2n - 1)}{n(n - 1)} \right] \quad (32)$$

Following Bond and Newton (Ref. 10), this quantity may be plotted against the inverse of:

$$K = -\frac{2x_2}{3} \quad (33)$$

For $x_2 = -1$, K becomes Hadamard's constant = $2/3$. In Figure 10 the non-dimensional radius $\bar{A} = A / \sqrt{\frac{\gamma}{g(\rho - \rho_1)}}$ is plotted against

$1/K$ using (32) and (33) and compared with Bond and Newton's corresponding experimental curve. It can be seen that the experimental values lie somewhat to the left of the theoretical ones, indicating that the drop attains circulation sooner than would have been expected from theory. The explanation for this may be sought in the fact that water is not entirely insoluble in castor oil, but that a gradual diffusion of water molecules takes place, particularly where the interfacial tension is low. The folding up of the surface layer is accordingly a statistical phenomenon which attains measurable proportions sometime before the local net interfacial tension becomes zero. The macroscopic concept gives merely a general qualitative picture of the phenomenon.

5.0 THE NATURE OF THE SURFACE LAYER

5.1 It was assumed in the above that a surface layer exists on droplets of a liquid suspended in another liquid or

in a gas, and that this layer is responsible for the formation of a stagnant sector on a part of the surface of the drop, which inhibits the action of the viscous surface traction in causing circulation of the drop. In attempting to answer the question as to the origin of this layer, an obvious possibility is an admixture of surface active molecules. These molecules, by virtue of their dual affinity, would resist submersion in either of the two liquids and would therefore tend to form a continuous layer which could only be liquidated by the above-mentioned process of "folding up". It is well known that the volume concentration of these molecules need only be very small to supply a sufficient quantity of molecules to form a monomolecular skin, but even so it is difficult to conceive that, in each case mentioned by Newton and Bond, foreign surface-active ingredients were, by some accident, present. Another possible mechanism of surface layer formation is that associated with the existence of an electrophoretic charge. It is known that the disperse phase in many emulsions exhibits an electrostatic charge, which attracts and binds oppositely charged ions, thus forming an electrical double layer. If one of the liquids is an insulator in which the ion concentration is low, molecular exchange between the surface layer and the bulk liquid will be rare, and hence the layer will exhibit the properties of a rigid skin. This possibility gains some support from an interesting observation of Garner's (Ref. 12), who found that circulation in drops is greatly promoted by certain salts diffusing from the drop outward into the surrounding medium. This suggests that the dissociated salt molecules by virtue of their ionic charge, neutralize the electrophoretic charge and thus destroy the incompressible double layer. It would therefore appear that circulation may be promoted by the same means as demulsification, i.e. coalescence of suspended liquid particles of an emulsion.

5.2 According to Bond and Newton the transition from the non-circulating to the circulating condition is governed by the non-dimensional number (3). It is shown in their paper that a number of substances show good agreement with this scaling law, but that the agreement is not good in the case of air bubbles in liquids. Here the transition takes place invariably at lower radii. It seems therefore that the stagnant layer is liquidated by a different mechanism than that proposed here. In this connection a note by Stuke (Ref. 18) is of interest, in which it is shown that the drag of air bubbles in water may be materially affected by the presence of surface-active agents. The concentration of these substances at which a noticeable change in drag occurs is so low that the surface tension is virtually unchanged. Analysing Stuke's results it was found that if a trace of surface-active substances is added to the water, agreement with Bond and Newton's number (3) immediately improves. Hence, it may be assumed that the mechanism here proposed becomes effective as a result of the presence of surface-active molecules. The inhibition of circulation in the absence of these molecules must be ascribed to a different cause. It is known, for instance, that certain monomolecular layers cannot sustain compression indefinitely; beyond a certain compressive stress they fold up into a polymolecular film. (Frenkel, Ref. 19.) It is possible that in the case of air bubbles this formation of a polymolecular film occurs at a bubble radius below that required to invoke the mechanism described here. To decide this question, more experimental evidence is called for.

6.0 DISTORTION OF A DROP IN A GAS STREAM

6.1 The question of distortion of a liquid drop suspended in a gas stream has been considered by a number of workers; among others, by Hughes and Gilliland (Ref. 13), Spilhaus (Ref. 20) and Hirschfeld (Ref. 21). No attempt has so far

been made to calculate the distorted shape itself, distortion being limited in each case to a "distortion index" figure governing the change in drag as a result of distortion, or, by assuming the distorted shape to be an ellipsoid of revolution, to an excentricity parameter. In the following an attempt will be made to calculate the distorted shape more accurately.

6.2 It will be assumed that the distortion is small so that if the surface be represented by the radius vector as a function of the polar angle, products and higher powers of the distortion terms can be neglected. Moreover, all forces will be considered to remain unmodified by the distortion. Since the viscosity of the liquid drop is high compared with that of the surrounding atmosphere, circulation, if it exists, can also be neglected. Proceeding on similar lines as before, the surface is represented by the radius vector, viz.

$$r = A \left(1 + \sum_{n=0}^{\infty} a_n \cos n\theta \right) \quad (34)$$

The choice of a Fourier series rather than Legendre polynomials was taken since methods for dealing with the former are readily available. It can be shown that the principal curvature sum now becomes:

$$J = \frac{1}{A} \left(2 + \sum_0^{\infty} a_n n^2 \cos n\theta - 2 \sum_0^{\infty} a_n \cos n\theta + \cot\theta \sum_0^{\infty} n a_n \sin n\theta \right) \quad (35)$$

Making use of the formula (see H.B. Dwight, "Table of Integrals" p. 86):

$$\cot\theta \sin n\theta = \sum_{m=1}^n \cos (n - 2m)$$

the last term of (35) may be transformed into a cosine series. The forces opposing the action of surface tension are gravity and aerodynamic pressure. The former is given by:

$$g\rho_2 A (1 + \cos\theta)$$

For the aerodynamic pressure an expression will be used representing in Fourier series form the results from a pressure plot on the surface of a sphere in sub-critical flow carried out by Flachsbarth (Ref. 22). This pressure function is applicable with fair accuracy over a range of Reynolds numbers from 10^3 to 10^5 . It may be represented in the form:

$$\frac{p - p_0}{\frac{1}{2} \rho_1 U^2} = \sum_{n=1}^{\infty} c_n \cdot \cos n\theta \quad (36)$$

and the coefficients up to the index $n = 9$ are given in Table II.

TABLE II

| Index n | Coefficient c_n |
|---------|-------------------|
| 1 | 0.446 |
| 2 | 0.393 |
| 3 | 0.246 |
| 4 | 0.067 |
| 5 | -0.030 |
| 6 | -0.030 |
| 7 | 0.012 |
| 8 | 0.012 |
| 9 | 0.007 |

Thus the complete pressure balance equation now becomes:

$$2 + \sum_{n=0}^{\infty} a_n n^2 \cos n\theta - 2 \sum_{n=0}^{\infty} a_n \cos m\theta + \sum_{m=0}^{\infty} n a_n \sum_{m=1}^m \cos (n - 2m) \\ = -W \sum_{n=1}^{\infty} c_n \cos n\theta + V (1 + \cos\theta)$$

Here W is the Weber non-dimensional parameter given by $W = \frac{1}{2} \rho_1 U^2 A / \gamma$ and $V = \rho_2 g A^2 / \gamma$. The two densities are related through the coefficient of $\cos\theta$, the relation being:

$$\rho_2 = 0.2205 \cdot U^2 \rho_1 / gA$$

Moreover, the volume conservation condition (17) assumes the form:

$$a_0 = - \sum_{n=1}^{\infty} \frac{a_n^2}{1 - 4n^2}$$

Equating coefficients of equal order terms, the coefficients a_n may be found in terms of the Weber number W. They are compiled in Table III, in order of ascending index n.

TABLE III

| Index n | Coefficient a_n |
|---------|-------------------|
| 0 | -0.0310.W |
| 1 | - |
| 2 | -0.0920.W |
| 3 | -0.0257.W |
| 4 | -0.00413.W |
| 5 | +0.00156.W |
| 6 | +0.00081.W |
| 7 | -0.00019.W |
| 8 | -0.00014.W |
| 9 | -0.00010.W |

The coefficient of order unity does not contribute to distortion within this approximation, but only causes a bodily vertical displacement of the whole drop. It may therefore be omitted. It will be seen that in this treatment all coefficients are proportional to the Weber number, i.e. the type of distortion remains the same, while the amplitude is directly proportional to W . Thus W is a measure of the magnitude of the distortion, a fact already pointed out by Taylor (Ref. 2). It is also evident that the first-order approximation dealt with here does not yield a critical Weber number for breakup.

6.3 With the aid of (34) and Table III the shape of the distorted drop can be calculated. This has been done and the shape has been plotted for three different Weber numbers in Figure 11(a-c). Comparison with experimental results in a quantitative sense was not attempted, but photographs of droplets suspended in an air stream show a very similar general pattern. Figure 12 was taken from a cinefilm by D.K. Stiles taken in his vertical wind tunnel. It will be seen that the main features, i.e. general lenticular shape with dimple on the underside are reproduced by the theory.

6.4 Although no critical Weber number for breakup can be obtained from this treatment an interesting conclusion may be drawn, bearing upon the difference in behaviour of a drop in a steady and a transient air stream. Taylor, analysing experimental results obtained by Lane, Prewett and Edwards (Ref. 3), finds that the ratio U_1/U_2 between the critical transient air velocity for breakup and the critical steady air velocity varies between 0.95 for large drops to 0.69 and below for small ones. In Figure 13 these results were plotted against the drop radius A and it is found that the curve intersects the U_1/U_2 -axis at approximately 0.58. Taylor develops a theory which appears to be capable of accounting for values of this ratio of between 0.71 and 0.985, but is at variance with the values for small drop

radii. Taylor's theory is founded on the fact that if the drop be represented by a mass-and-spring system, then the distortion under a suddenly applied load is twice that under a steady load. For small drop radii the inertia forces may be expected to become insignificant relative to surface tension and aerodynamic forces. Hence for small droplets a different explanation may be suggested. It is well known that if the motion of a solid body in a fluid be started impulsively from rest, or if the fluid motion be turned on suddenly, the ensuing flow is initially purely potential, the boundary layer being developed gradually. Hence, a droplet in a transient blast of air may be considered to be subjected initially to potential streaming only. On this assumption the previous treatment may be repeated, replacing (36) by the expression:

$$\frac{p - p_0}{\frac{1}{2} \rho_1 U^2} = -\frac{1}{8} + \frac{9}{8} \cos 2\theta$$

It will be seen that the series in (34) now reduces to the finite term:

$$r = A \left(1 - \frac{3W}{32} - \frac{9W}{32} \cos 2\theta \right) \quad (37)$$

To find the appropriate value for U_1/U_2 , the following argument will be taken: Although the present treatment does not hold for large distortion, it may be assumed that when the distortion reaches the stage where front and rear stagnation point of the drop coincide, the resulting toroidal shape will prove unstable and disintegration of the drop will proceed spontaneously. This is borne out by Rayleigh's work on the instability of liquid columns under surface tension. Thus, breakup will be assumed to take place when:

$$r_{\theta=0} + r_{\theta=\pi} = 0$$

In the transient case (37) this condition is fulfilled provided that $W_1 = 2.67$ whereas, in the case of a steady air stream (34), $W_2 = 8.17$. Hence it will be found:

$$\frac{W_1}{W_2} \doteq 0.327 \quad \text{or} \quad \frac{U_1}{U_2} = 0.570$$

This figure for U_1/U_2 compares well with the extrapolated experimental value of 0.58. It may be concluded that very small drops in a transient air blast are broken up by the potential phase of the motion which is more efficient in distorting the drops than the wake motion. This may account for the relative efficiency of alternating air flow (ultrasound) in atomizing a liquid.

From the value 8.17 for W_2 it may be seen that the first order approximation for the critical Weber number compares poorly with Lane, Prewett and Edwards' experimental value of 2.7.

7.0 CONCLUSIONS

7.1 Experiments were carried out to clarify the views held regarding this mechanism of suppression of circulation in drops of liquid moving through a liquid medium. It was shown that both the theories of surface viscosity and local change of surface energy cannot be correct and an alternative theory of the phenomenon of transition from the circulating to the non-circulating drop was put forward. This theory was shown to give an adequate representation of the vortex motion in the drop, but the value for the critical drop radius for transition was found to be somewhat higher than experimental values. This may be ascribed to the fact that transition is probably a statistical phenomenon, for which macroscopic hydrodynamics can only be expected to provide an approximation.

The existence of an incompressive surface layer may be shown by experiment and an attempt was made to explain its appearance in falling drops. From the extent of the surface layer the drag of the drop may be calculated with fair accuracy. The theory also accounts for the appearance of a thin filament of drop material in the wake.

7.2 A theoretical treatment was developed to account for the shape of the drop when suspended in an air stream or falling through still air. The general shape of the droplet agrees with the observed distortion, but being a first order approximation the theory is unable to give an exact value for the critical radius for breakup of the drop. The ratio between the critical velocities for breakup in a transient and in a steady airstream can, however, be predicted with fair accuracy, at least for small drops. In this sense this theory supplies a sequel to G.I. Taylor's theoretical analysis of experimental results obtained by Lane, Prewett and Edwards.

8.0 REFERENCES

1. Kronig, R.
Brink, J.C. On the theory of extraction from falling droplets. Applied Sci. Research, v. A2, n. 2, pp. 142-154, 1950.
2. Taylor, G. The shape and acceleration of a drop in a high speed air stream. MOS CDES (Chemical Defence Experimental Station) Porton, England, 6600/5278/49.
3. Lane, W.R.
Prewett, W.C.
Edwards, J. Unpublished Ministry of Supply Reports.
4. Golitzine, N. Unpublished work of the Division of Mechanical Engineering, National Research Council (Canada).
5. Hadamard, M.J. Mouvement permanent lent d'une sphere liquide et visqueuse dans un liquide visqueux. Académie des Sciences, Comptes Rendus, v. 152, pp. 1735-1738, 1911.

6. Rybczynsky, D.P. Bull Acad. Sci., Cracow (A) 403, 1911.
Referred to in Sir H. Lamb's "Hydrodynamics", 6th edition, p. 600,
Cambridge Univ. Press.
7. Arnold, H.D. Limitations imposed by slip and
inertia terms upon Stokes' Law for
the motion of spheres through liquids.
Philosophical Magazine, ser. 6, v. 22,
pp. 755-775, 1911.
8. Boussinesq, J. Sur l'existence d'une viscosité super-
ficielle, dans la mince couche de
transition séparant un liquide d'un
autre fluide contigu.
Ann. Chem. Phys., v. 29, pp. 349-357, 1913.
9. Bond, W.N. Bubbles and drops and Stokes' Law.
Philosophical Magazine, ser. 7, v. 4,
pp. 889-898, 1927.
10. Bond, W.N.
Newton, D.A. Bubbles, drops and Stokes' Law
(Paper 2).
Philosophical Magazine, ser. 7, v. 5,
pp. 794-800, 1928.
11. Weyssenhoff, J. Betrachtungen über den Gültigkeits-
bereich der Stokesschen und der
Stokes-Cunninghamschen Formel I.
Hydrodynamischer Teil.
Annalen der Physik, 4th series, v. 62,
pp. 1-45, 1920.
12. Garner, F.H. Diffusion mechanism in the mixing of
fluids.
Institution of Chemical Engineers,
Trans., v. 28, pp. 88-96, 1950.
13. Hughes, R.R.
Gilliland, E.R. The mechanics of drops.
Heat Transfer and Fluid Mechanics
Institute.
Preprints of papers held at Stanford
University, June 20-22, 1951. See
pp. 53-72.
14. Spells, K.E. Study of circulation patterns within
liquid drops moving through liquid.
Phys. Soc. Proc., v. 65, n. 391B,
pp. 541-546, July 1, 1952.

15. Hagerty, P.F. S.M. Thesis Chem. Eng. Pract. M.I.T., 1947.
16. Lamb, Sir.H. Hydrodynamics, 6th edition. Cambridge Univ. Press, p. 594, para. 335, 1932.
17. Magnus, W.
Oberhettinger, F. Formulas and theorems for the special functions of mathematical physics. Chelsea Publishing Co., New York, p. 76, 1949.
18. Stuke, B. Das Verhalten der Oberfläche von sich in Flüssigkeiten bewegendenden Gasblasen. Naturwissenschaften, v. 39, n. 14, pp. 325-326, 1952.
19. Frenkel, I.I. Kinetic theory of liquids. The Clarendon Press, Oxford, 1946.
20. Spilhaus, A.F. Raindrop size, shape and falling speed. J. Met., v. 5, pp. 108-110, 1948.
21. Hitschfeld, W. Free fall of drops through air. Trans. Amer. Geoph. Union, v. 32, n. 5, pp. 697-700, 1951.
22. Flachsbart, O. Neue Untersuchungen über den Luftwiderstand von Kugeln. Phys. Zeit, v. 28, pp. 461-469, 1927.
23. Ramsey, A.S. A treatise on hydromechanics. G. Bell, London, para. 13.8, 1942.
24. Carslaw, H.S.
Jaeger, J.C. Operational methods in applied mathematics. Clarendon Press, Oxford, para. 29, p. 72, 1941.



FIG. 1

DROP DIAM. 1.77 CM.
FALLING SPEED 1.16 CM/SEC.
EXPOSURE 1/2 SEC.



FIG.2

DROP DIAM. 1.21 CM.
FALLING SPEED 0.62 CM/SEC
EXPOSURE 1 SEC.

WATER DROP IN CASTOR OIL

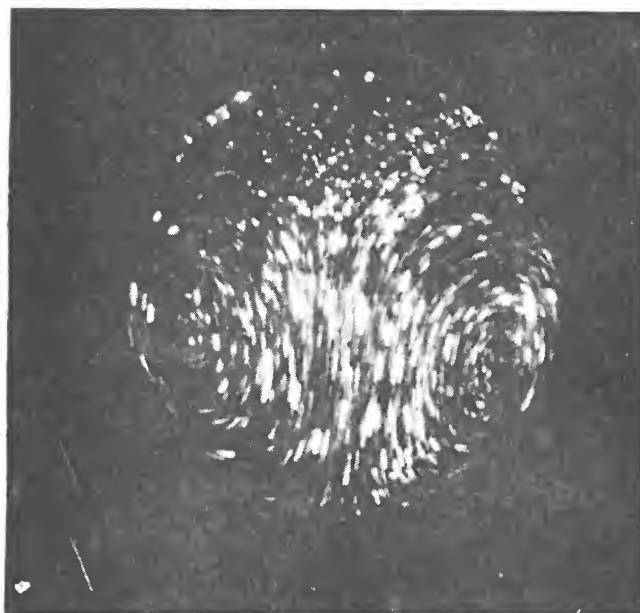


FIG. 3

DROP DIAM. 0.97 CM.
FALLING SPEED 0.25 CM/SEC.
EXPOSURE 1 SEC.

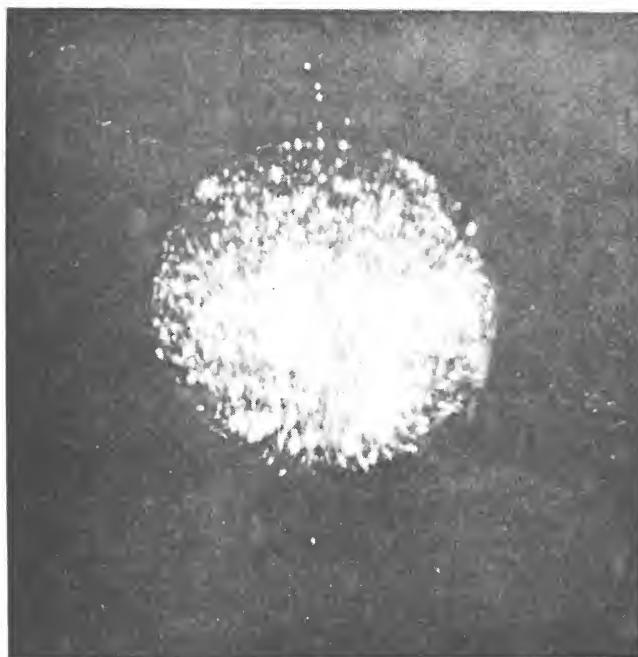
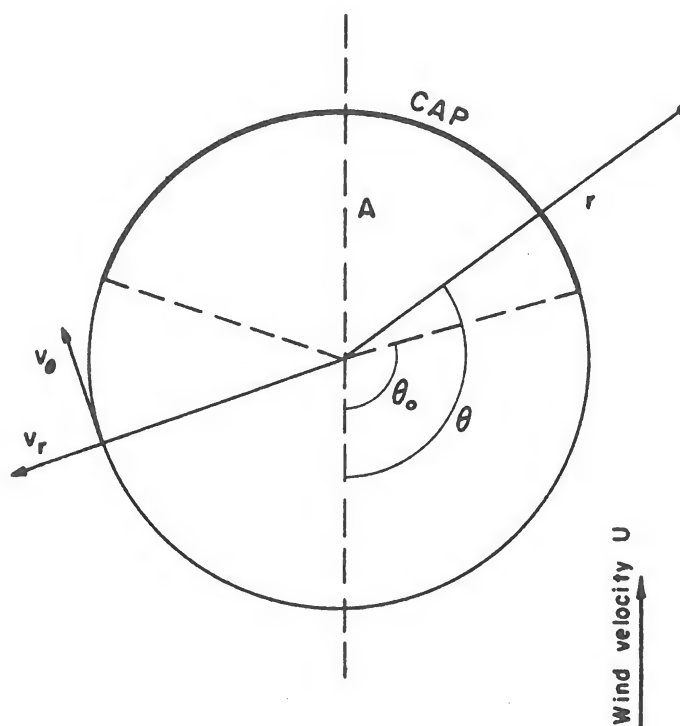


FIG. 4

DROP DIAM. 0.74 CM.
FALLING SPEED 0.13 CM/SEC.
EXPOSURE 1 SEC.

WATER DROP IN CASTOR OIL



SPHERICAL CO-ORDINATES OF DROP

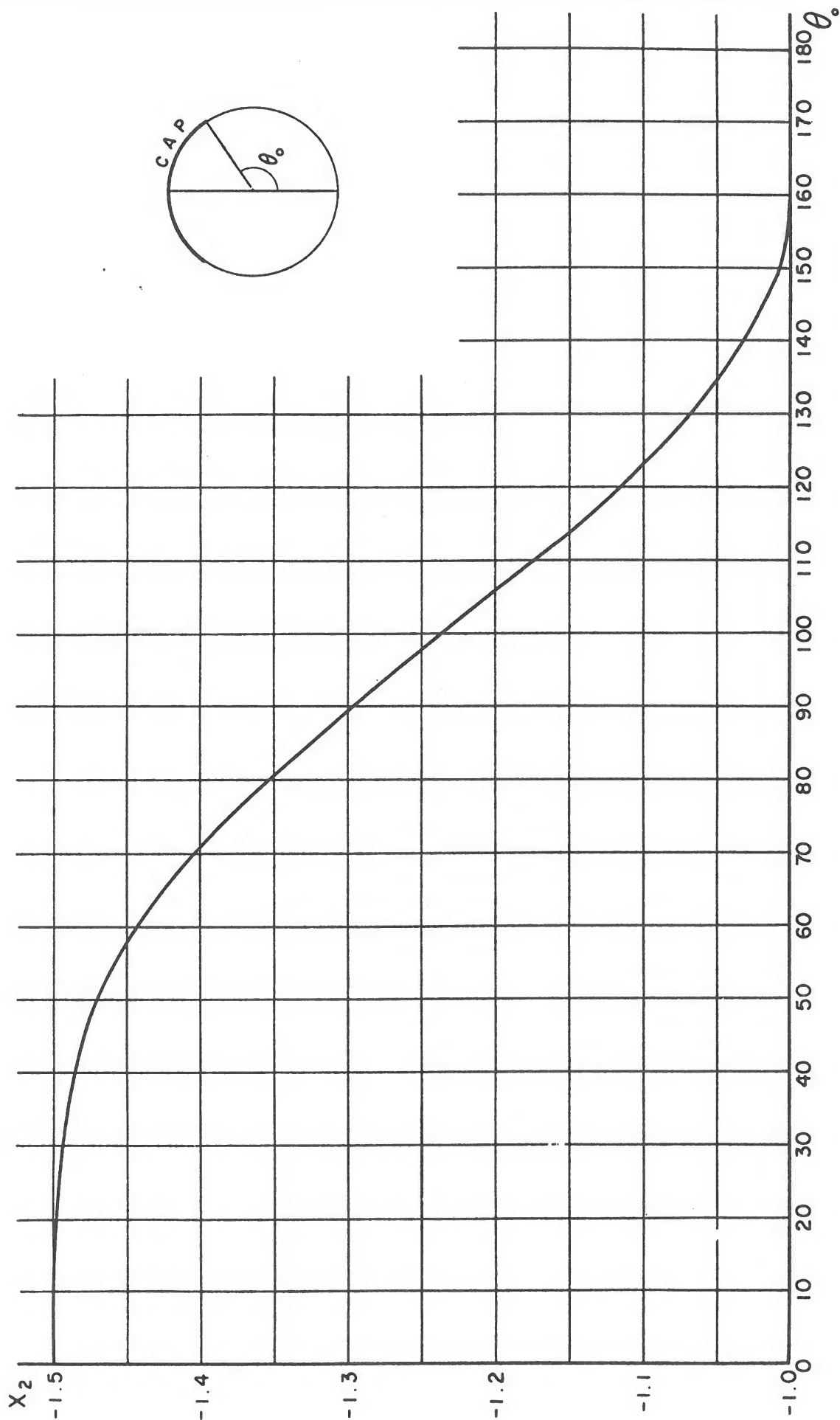


FIG. 6
MT-22

DEPENDENCE OF TOTAL DRAG ON CENTRAL ANGLE OF STAGNANT CAP

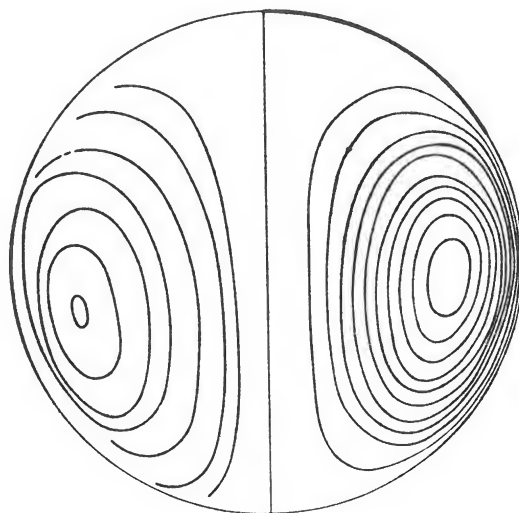


FIGURE 7

COMPARISON OF ACTUAL AND THEORETICAL STREAMLINES

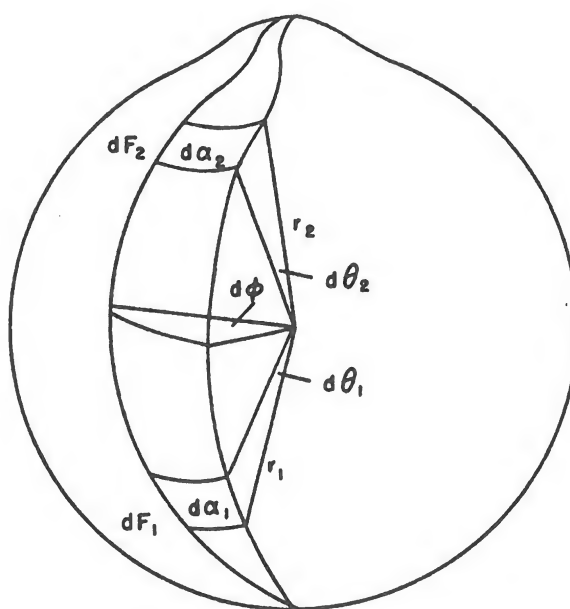
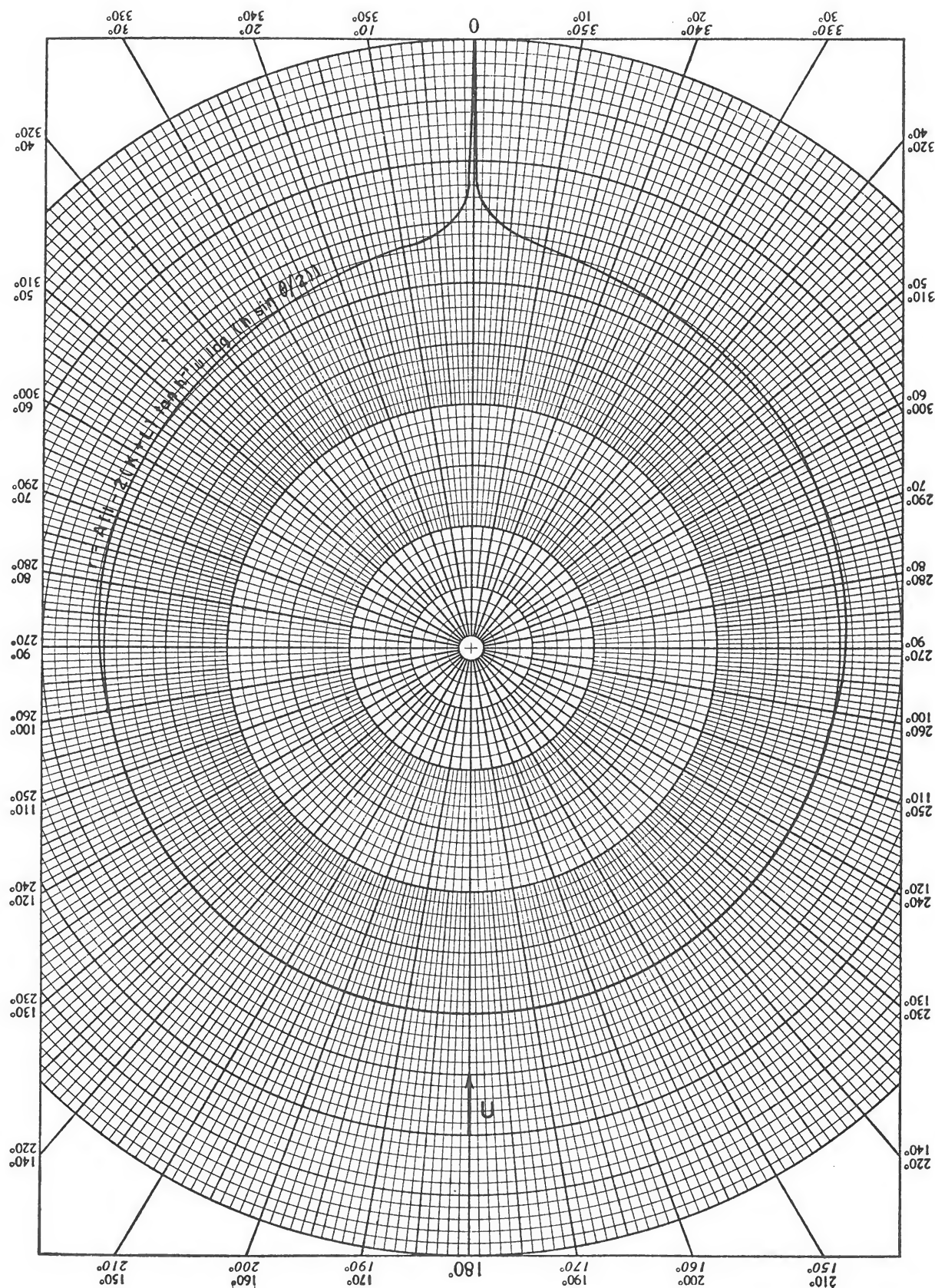


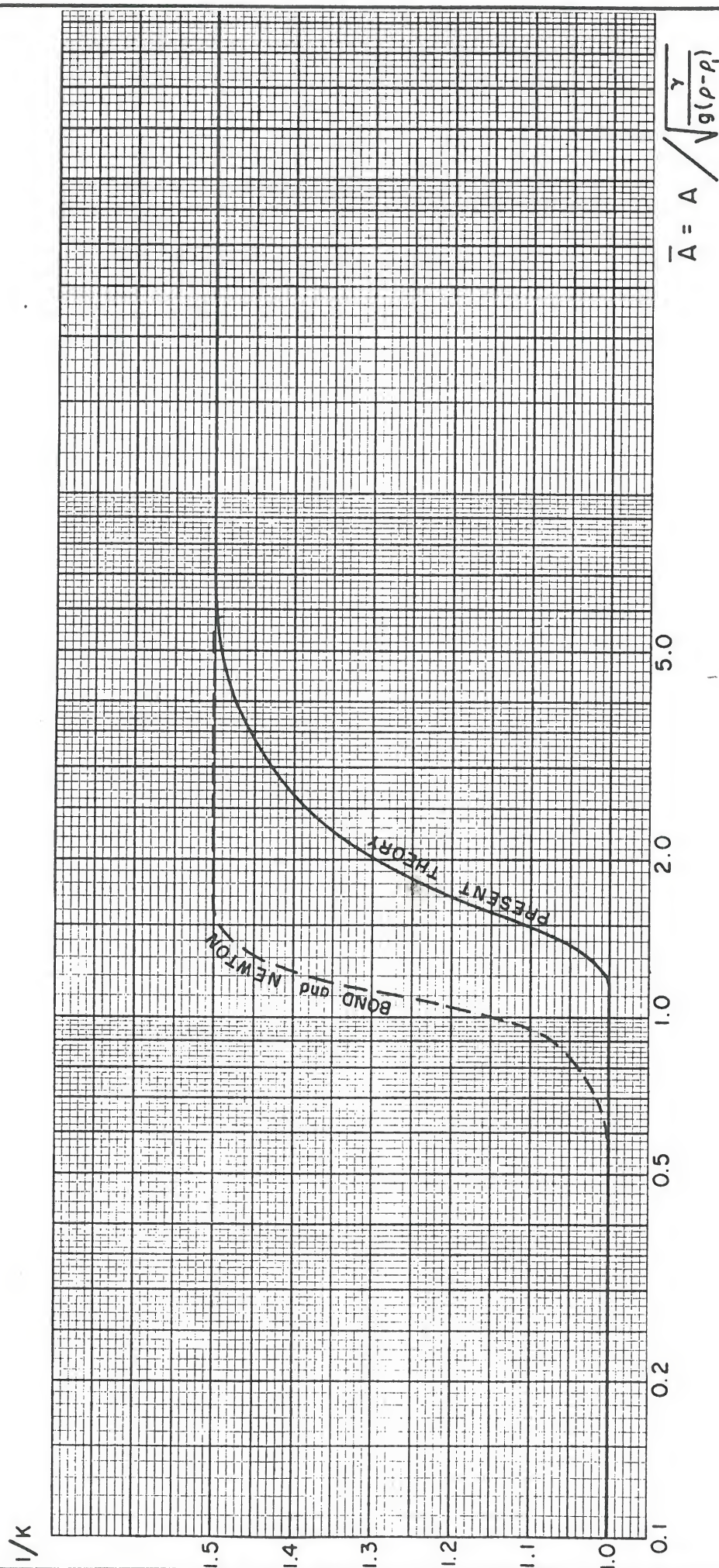
FIGURE 8

SURFACE FORCES ON DISTORTED DROP

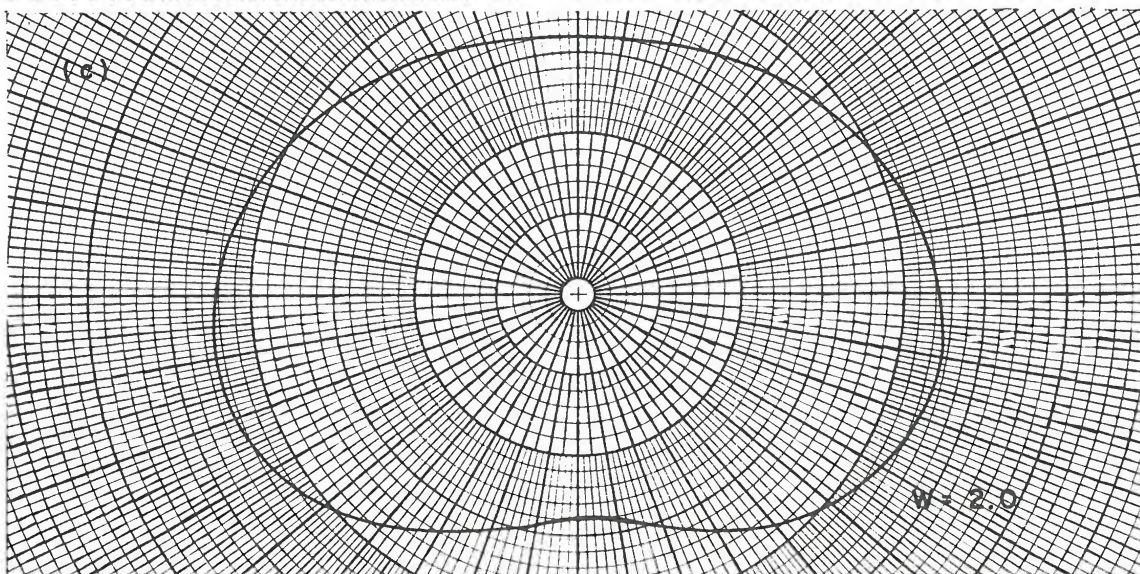
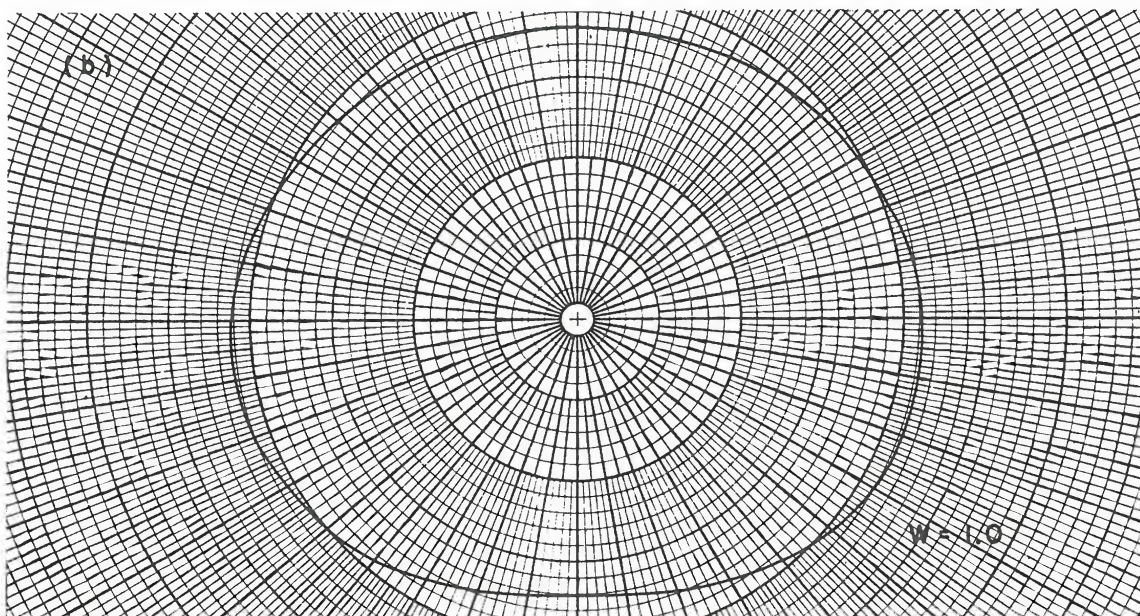
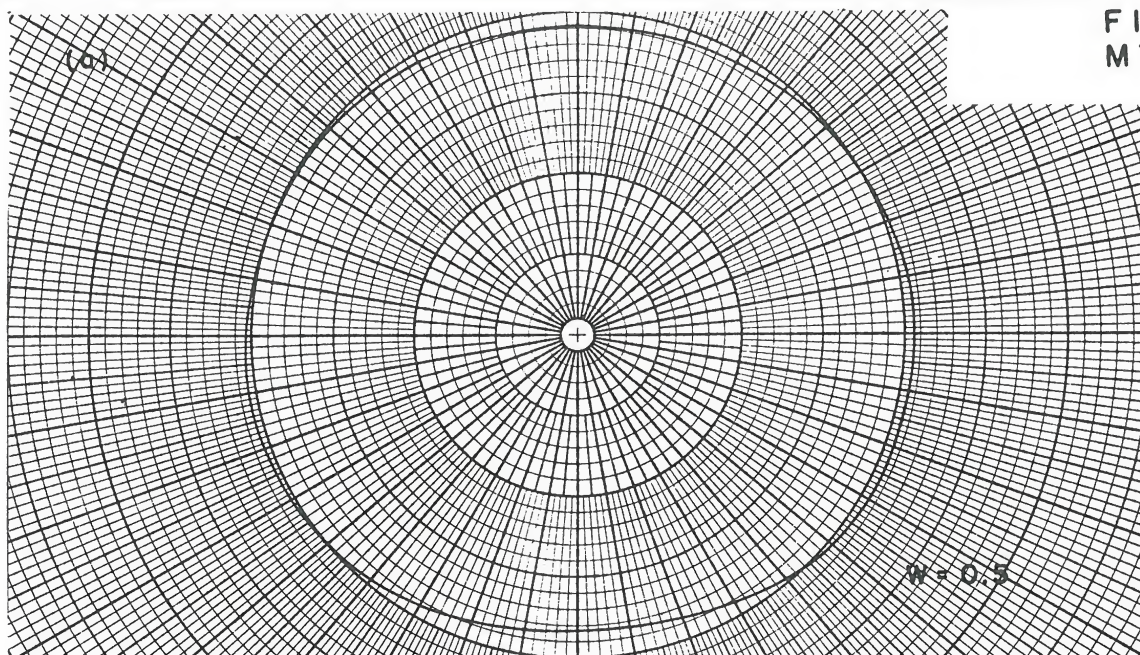
FIG. 9
MT - 22



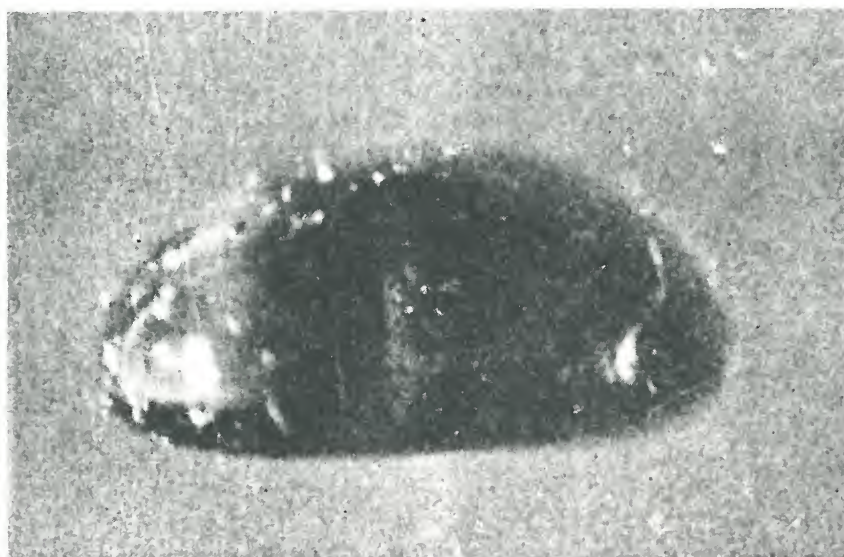
INSTABILITY OF SURFACE LAYER AROUND REAR STAGNATION POINT



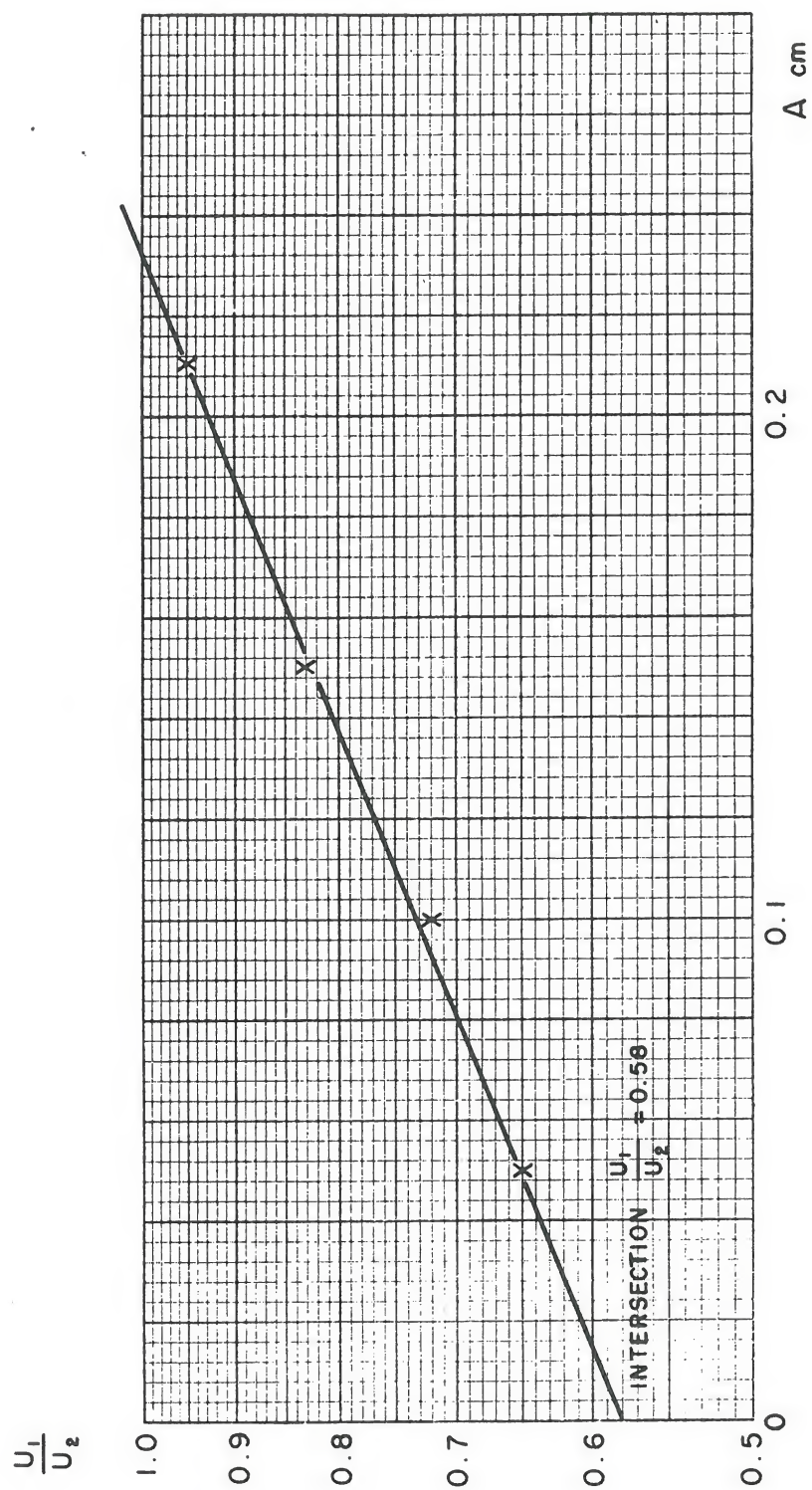
HADAMARD'S CONSTANT VS NON-DIMENSIONAL RADIUS
COMPARISON BETWEEN THEORY AND EXPERIMENT



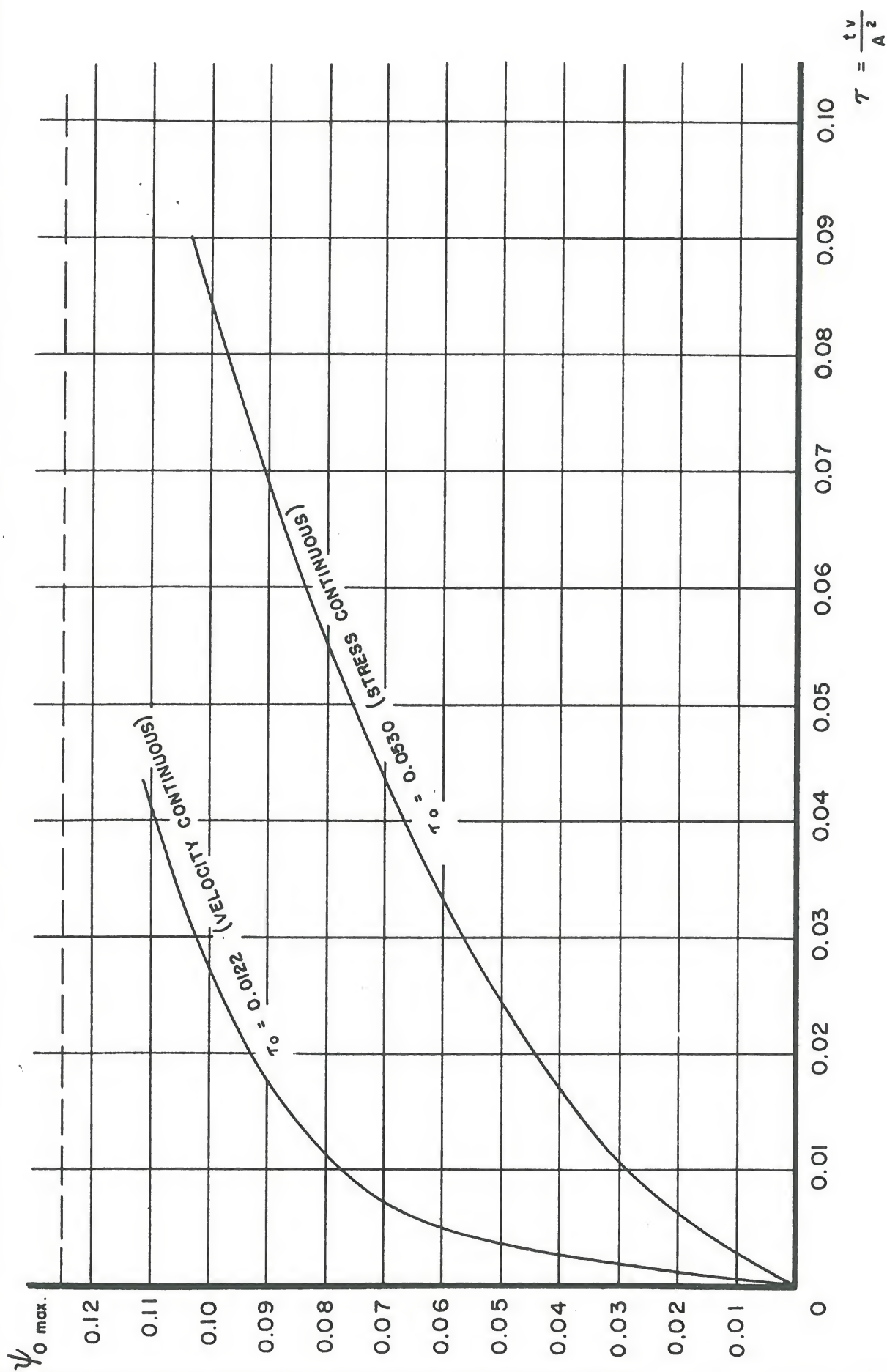
DISTORTION OF A DROP IN A GAS STREAM FOR THREE WEBER NUMBERS



DISTORTED DROP SUSPENDED IN VERTICAL WIND TUNNEL



DEPENDENCE OF BREAKUP VELOCITY RATIO ON DROPLET RADIUS



GROWTH OF STRENGTH OF CIRCULATION FROM REST WITH NON-DIMENSIONAL TIME

APPENDIX A

DEVELOPMENT OF CIRCULATION FROM REST BY VISCOUS SHEAR IN THE VICINITY OF A DROP

It is assumed that the drop is projected with uniform velocity U into a shearing atmosphere. Two extreme cases will be considered here: (1) The viscous resistance of the drop is negligible compared with the viscosity of the surrounding medium (gas bubbles in liquids), the surface traction on the drop can therefore be taken as zero. (2) The viscosity of the surrounding medium is small compared with that of the drop (liquid drops in air), i.e. the surface shear stress is continuous across the boundary of the drop.

A.1 CONTINUOUS SURFACE VELOCITY (= TANGENTIAL VELOCITY OF EXTERNAL FLUID)

Stokes' stream function ψ may be shown to be determined by the differential equation (Ref. 23):

$$\left(\frac{\partial^2}{\partial r^2} + \frac{(1 - y^2)}{r^2} \frac{\partial^2}{\partial y^2} - \frac{1}{\nu} \frac{\partial}{\partial t} \right) \left(\frac{\partial^2}{\partial r^2} + \frac{(1 - y^2)}{r^2} \frac{\partial^2}{\partial y^2} \right) \psi = 0$$

here ν is the kinematic viscosity of the drop, r the radius vector and $y = \cos\theta$ where θ is the polar angle, and t the time. Putting $\psi = \psi_0 (1 - y^2)$, this equation may be written as:

$$\left(\frac{\partial^2}{\partial r^2} - \frac{2}{r^2} - \frac{1}{\nu} \frac{\partial}{\partial t} \right) \left(\frac{\partial^2}{\partial r^2} - \frac{2}{r^2} \right) \psi_0 = 0 \quad (\text{A.1})$$

Put: $\left(\frac{\partial^2}{\partial r^2} - \frac{2}{r^2} \right) \psi_0 = v$ and $\left(\frac{\partial^2}{\partial r^2} - \frac{2}{r^2} - \frac{1}{\nu} \frac{\partial}{\partial t} \right) v = 0$

and apply the Laplace transformation: $\bar{v} = \int_0^{\infty} e^{-pt} v \, dt$.

leading to:

$$\left(\frac{\partial^2}{\partial r^2} - \frac{2}{r^2} - \frac{p}{v} \right) \bar{v} = 0 \quad (\text{A.2})$$

A solution of (A.2) which is finite at the origin is:

$$\bar{v} = \sqrt{r} J_{3/2} \left(ir \sqrt{\frac{p}{v}} \right)$$

where $J_{3/2}$ is the Bessel function of order $3/2$.

Hence, the complete solution is

$$\bar{\psi}_0 = Cr^2 + B \sqrt{r} J_{3/2} \left(ir \sqrt{\frac{p}{v}} \right) \quad (\text{A.3})$$

where $\bar{\psi}_0$ is the transform of ψ_0 , and C and B are constants to be determined by the boundary conditions. These are:

- (a) The radial velocity must vanish at the boundary of the drop: $(\bar{\psi}_0)_{r=A} = 0$.
- (b) The expression $v_{\theta} \sin \theta$ at $r = A$ must be a constant in time, i.e.

$$\frac{1}{A} \left(\frac{\partial \bar{\psi}_0}{\partial r} \right)_{r=A} = \frac{s}{p}$$

where s is a constant which may be determined from the steady state solution.

Expressing $J_{3/2}$ by its corresponding hyperbolic functions (see Ref. 17, p. 18) these conditions may be put into the form:

$$CA^2 + BY = 0 \quad \text{and} \quad 2C + BY^*/A = s/p$$

where:

$$Y = \left(\frac{p}{v}\right)^{-\frac{1}{4}} \left(\frac{\sinh A \sqrt{\frac{p}{v}}}{A \sqrt{\frac{p}{v}}} - \cosh A \sqrt{\frac{p}{v}} \right)$$

and $Y' = dY/dA$. From this the constants B and C are determined as:

$$B = \frac{A^2 s}{p (AY' - 2Y)}$$

$$C = - \frac{sAY}{p (AY' - 2Y)}$$

The complete solution for the transformed stream function is therefore:

$$\bar{\psi}_0 = \frac{sA^3}{rp} \frac{\sinh r\sqrt{\frac{p}{v}} - r\sqrt{\frac{p}{v}} \cosh r\sqrt{\frac{p}{v}} - (r^3/A^3) (\sinh A\sqrt{\frac{p}{v}} - A\sqrt{\frac{p}{v}} \cosh A\sqrt{\frac{p}{v}})}{3A\sqrt{\frac{p}{v}} \cosh A\sqrt{\frac{p}{v}} - 3 \sinh A\sqrt{\frac{p}{v}} - A^2 \left(\frac{p}{v}\right) \sinh A\sqrt{\frac{p}{v}}}$$

(A.4)

Using the Mellin inversion integral (Ref. 24) the original stream function may be found by the method of residues. The function (A.4) has a double pole at the origin $p = 0$. The residue of this pole is:

$$\frac{sr^2}{2A^2} (r^2 - A^2)$$

Other simple poles exist at the zeros of the function:

$$3x_n \cos x_n - 3 \sin x_n + x_n^2 \sin x_n = 0$$

or alternatively:

$$\tan x_n = \frac{3x_n}{3 - x_n^2} \quad (A.5)$$

The residues here are of the form:

$$\left[\frac{2r^2}{x_n^2} - \frac{2A^3 (\sin qx_n - qx_n \cos qx_n)}{x_n^2 r (\sin x_n - x_n \cos x_n)} \right] s.e^{-x_n^2 vt/A^2} \quad \text{where } q = r/A$$

Hence, the inverted stream function now becomes:

$$\psi_0 = sA^2 \left\{ \frac{q^2 (q^2 - 1)}{2} - \sum_{n=1}^{\infty} \frac{2}{x_n^2} \left[\frac{(\sin x_n q - x_n \cos x_n q)}{q (\sin x_n - x_n \cos x_n)} - q^2 \right] e^{-x_n^2 vt/A^2} \right\} \quad (A.6)$$

It will be seen from equation (A.6) that the steady state is approached as $t \rightarrow \infty$. From (13) of the text it may be concluded that the value of the constant s must be:

$$s = U/2.$$

The first four solutions of (A.5) are tabulated below:

| n | x_n |
|-----|--------|
| 1 | 5.765 |
| 2 | 9.095 |
| 3 | 12.325 |
| 4 | 15.515 |

A.2. CONTINUOUS SURFACE STRESS (= SURFACE TRACTION OF EXTERNAL FLUID)

A.2.1 The treatment follows on similar lines as under Section A.1, but it is now assumed that due to the relatively high viscosity of the droplet fluid the circulation is so slow that the surface shear stress may be considered independent of

time. Thus, boundary condition (b) of the previous paragraph must be replaced by:

(b') The expression $p_{r\theta} \sin\theta$ at $r = A$ must be a constant in time, i.e.:

$$\left(\frac{\partial^2 \bar{\psi}_0}{\partial r^2} \right)_{r=A} \frac{1}{A} - \left(\frac{\partial^2 \bar{\psi}_0}{\partial r} \right)_{r=A} \frac{1}{A^2} = \frac{s'}{p}$$

Proceeding as before, the constants in (A.3) are determined from the boundary conditions, and it is found that:

$$\bar{\psi}_0 = \frac{s'A^4}{rp} \cdot \frac{\sinh rp' - rp' \cosh rp' - q^3 (\sinh Ap' - Ap' \cosh Ap')}{3 \sinh Ap' - 3Ap' \cosh Ap' + 2(Ap')^2 \sinh Ap' - (Ap')^3 \cosh Ap'} \quad (A.7)$$

where $p' = \sqrt{\frac{p}{v}}$.

Inverting this expression in the usual way it is found that the double pole at the origin has the residue:

$$\frac{s'A^3 q^2 (q^2 - 1)}{8}$$

whereas an infinitude of simple poles exists at the roots of:

$$\tan x'_n = x'_n \frac{3 - x_n'^2}{3 - 2x_n'^2} \quad (A.8)$$

Hence, the inverted stream function becomes:

$$\psi_0 = \frac{s'A^3}{8} \left\{ q^2 (q^2 - 1) - 16 \sum_{n=1}^{\infty} \frac{q^{-1} (\sin x'_n q - x'_n q \cos x'_n q) - q^2 (\sin x'_n - x'_n \cos x'_n)}{x_n'^2 (\sin x'_n - x'_n \cos x'_n + x_n'^2 \sin x'_n)} e^{\frac{-x_n' t v}{A^2}} \right\} \quad (A.9)$$

The constant s' may again be determined from the steady state problem of Hadamard's (Ref. 5) where it is found that:

$$s' = 2U\eta_1/A\eta_2$$

where η_1 is the viscosity of the medium and η_2 the viscosity of the drop. The first four roots of the transcendental (A.8) are given in the following table.

| n | x_n |
|---|--------|
| 1 | 4.232 |
| 2 | 7.588 |
| 3 | 10.810 |
| 4 | 13.898 |

A.2.2 In order to obtain an estimate of the rate at which circulation is established, the intensity of circulation will be defined, following Hughes and Gilliland (Ref. 13), as the flow encompassed by the circular vortex ring. This is proportional to the maximum of the stream function ψ_0 . This maximum was determined graphically from (A.6) and (A.9) and is shown plotted against non-dimensional time in Figure 14. From this, the time t_0 required to reach e^{-1} of full circulation is respectively:

$$t_0 = 0.0122 \frac{A^2}{\nu} \quad \text{for continuous velocity}$$

$$t_0 = 0.0530 \frac{A^2}{\nu} \quad \text{for continuous shear stress}$$

It follows that if, for example, a drop of water is projected into air, the time required to establish circulation is over

four times that needed to reach circulation were it dropped into, say, a heavy oil.

A.2.3 As an example, consider a drop of kerosine of, say, 50 microns radius entering an air stream. Assuming the continuous shear condition to hold and with a kinematic viscosity of the fuel of 0.01 stokes, the time t_0 is found to be of the order of 100 microseconds. As this is of smaller order than the observed ignition delay, it follows that circulation may be a factor to be reckoned with in assessing this delay.